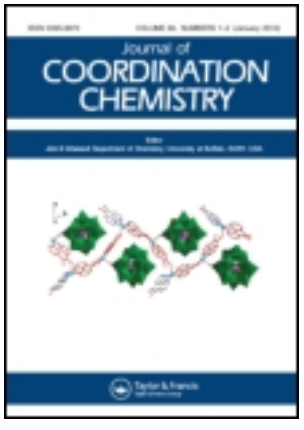

Journal of Coordination Chemistry
Publication details, including instructions for authors and subscription information:
http://www.tandfonline.com/loi/gcoo20

Review: protonation, complex-formation equilibria, and metal-ligand interaction of salicylaldehyde Schiff bases

Ahmed A. El-Sherif[ab] & Mutlaq S. Aljahdali[c]

[a] Faculty of Science, Department of Chemistry, Cairo University, Cairo, Egypt

[b] Faculty of Arts and Science, Department of Chemistry, Northern Border University, Rafha, Saudi Arabia

[c] Faculty of Science, Department of Chemistry, King Abd Al-Aziz University, Jeddah, Saudi Arabia

Published online: 22 Oct 2013.

To cite this article: Ahmed A. El-Sherif & Mutlaq S. Aljahdali (2013) Review: protonation, complex-formation equilibria, and metal-ligand interaction of salicylaldehyde Schiff bases, Journal of Coordination Chemistry, 66:19, 3423-3468, DOI: 10.1080/00958972.2013.839027

To link to this article: http://dx.doi.org/10.1080/00958972.2013.839027

Journal of Coordination Chemistry, 2013
Vol. 66, No. 19, 3423–3468, http://dx.doi.org/10.1080/00958972.2013.839027

Review: protonation, complex-formation equilibria, and metal–ligand interaction of salicylaldehyde Schiff bases

AHMED A. EL-SHERIF*†‡ and MUTLAQ S. ALJAHDALI§

†Faculty of Science, Department of Chemistry, Cairo University, Cairo, Egypt
‡Faculty of Arts and Science, Department of Chemistry, Northern Border University, Rafha, Saudi Arabia
§Faculty of Science, Department of Chemistry, King Abd Al-Aziz University, Jeddah, Saudi Arabia

(*Received 2 May 2013; accepted 1 August 2013*)

Schiff bases (SBs) are aldehyde- or ketone-like compounds in which the carbonyl group is replaced by an imine or azomethine. In spite of the large interest always shown in the coordination properties of Schiff base ligands and the attention paid in recent years to the possible variable biological activities of their metal complexes, studies dealing with protonation and formation equilibria of Schiff bases and their complexes are still very rare. Thus, the importance of the determination of the equilibrium constants of Schiff bases and their complex formation equilibria is of paramount importance to understand the complicated biological reactions like transamination, racemization and decarboxylation. The 33 ligands considered herein include salicylaldehyde/substituted salicylaldehyde SBs and salicylaldehyde/substituted salicylaldehyde amino acid SBs. This article is focused on protonation and complex-formation equilibria of salicylaldehyde or substituted salicylaldehyde SBs and salicylaldehyde amino acid SBs in aqueous and nonaqueous solutions, taking into account also the structure-activity correlation of SBs and their metal(II) complexes based on their stability constants. Activity of SBs enhances upon complexation and the order of activity is nearly in accord with the order of the formation constants of metal ions. The few enthalpy and entropy changes available for such protonation and complex-formation reactions are reported and discussed.

Keywords: Schiff bases; Protonation equilibria; Complex formation; Salicylaldehyde; Amino acid Schiff bases

1. Introduction

Schiff bases (SBs) are important intermediates in a number of enzymatic reactions involving enzyme interaction with an amino or a carbonyl group of a substrate. SBs are derived by condensation of primary amines and an active carbonyl group [1–3]. They form stable complexes with metal ions, especially if the amine and carbonyl compounds contain a second functional group sufficiently near the site of condensation to form five- and/or six-membered chelate rings. Metal chelation is involved in many important biological processes where coordination can occur between a variety of metal ions and a wide range of ligands. In bioinorganic chemistry, interest in Schiff-base complexes derives from their ability to provide synthetic models for metal-containing sites in metalloproteins and their contribution in

*Corresponding author. Email: aelsherif72@yahoo.com

developments of medicinal chemistry. Thus, SBs and their complexes have a variety of applications in biological, clinical, and analytical fields [4, 5]. Metal complexes with SBs have attracted attention due to remarkable antifungal [6], antibacterial [7, 8], and antitumor activities [9, 10]. Data related to protonation constants of biologically active ligands will be valuable in further understanding of their chemistry in biological systems. Also, knowledge of equilibrium constants of some compounds is necessary for calculation of the concentration of each ionized species at any pH, which is important for understanding of the physiochemical behavior of such molecules [11]. With this in mind and in continuation of our research program directed to study the protonation and complex-formation equilibria of biologically active compounds [12–18], the present review investigates the protonation, complex-formation equilibria and coordination properties of salicylaldehyde SBs and their derivatives to give a picture of their ionization and interaction with metal ions. Moreover, the effect of complexation on the biological activity of SB ligands will be discussed.

2. Schiff bases

2.1. *History*

Hugo Schiff was a German chemist born in 1834 in Frankfurt. In 1879, he founded the chemical institute of the University of Florence and discovered SBs and the Schiff test named after him. In the University of Florence, the Hugo Schiff international store house exists today.

2.2. *Formation of SBs*

SBs, so called since their synthesis was first reported by Schiff [19], result from condensation of primary amines with aldehydes and ketones forming a >C=N double bond as shown in scheme 1. The interaction of the resulting imines ($R_1R_2C{=}N{-}R_3$ or $R_1HC{=}N{-}R_3$) with metal ions occurs via nitrogen lone pair electrons. The SBs are formed with ketones less readily than with aldehydes.

SBs decompose or polymerize rapidly unless there is at least one aryl group bonded to nitrogen or carbon of the >C=N double bond [20]. Therefore, SBs that contain aryl substituents are substantially more stable and more readily synthesized, while those which contain alkyl substituents are relatively unstable. SBs of aliphatic aldehydes are relatively unstable and readily polymerizable [21, 22] while those of aromatic aldehydes having effective conjugation are more stable [23, 24].

2.3. *Formation of SBs by template method*

Synthesis of many compounds is difficult or even impossible by common methods which have been synthesized by the template process. There is no strict definition of a template

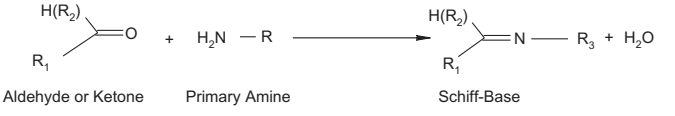

Scheme 1. Formation of SBs.

reaction (scheme 2). One definition is: "Template processes are those in which the metal ion, or another center that has a definite stereochemistry and electronic state, serves as a mold or pattern for forming, from appropriate building blocks" [25]. The template effect of metals is twofold: (i) polymerization reactions are suppressed, since the local concentration of reactants around the metal is very high; and (ii) multi-step reactions are possible, since the metals hold the reactants together. Accumulated experimental data show that the yield of the template reaction is sensitive to a number of factors including order and timing of reagent addition, hydrogen ion concentration, anion of metal salts, solvent, and temperature. It has been postulated that either (i) organic intermediate or (ii) the product ligand must be formed prior to the point where the metal salt is added or (iii) the coordination of the organic precursors occurs.

Systematic study of the mechanism has shown that Schiff-base formation depends strongly on the mixing order of reactants. The equilibrium is achieved most rapidly when the metal is added at the end of the reaction [26].

Coordination of the Schiff base has two effects: (i) facilitating removal of the NH protons and (ii) enhancing nucleophilic attack at the carbon of the carbonyl group.

2.4. *SBs as ligands for coordination*

SBs are important intermediates in a number of enzymatic reactions involving enzyme interaction with an amino or carbonyl of a substrate. In bioinorganic chemistry, interest in Schiff-base complexes derives from their ability to provide synthetic models for metal-containing sites in metalloproteins and to contribute to medicinal chemistry. Thus, SBs and their complexes have a variety of applications in biological, clinical, and analytical fields. Bearing the excellent electron-donor >C=N imino, they can form various complexes with a wide range of metals including main group, transition, and lanthanide metals.

2.5. *General information about the determination of equilibrium data*

A problem which is generally encountered in compiling a collection of thermodynamic equilibria data is that the data are difficult to compare because they come from different sources and have been obtained under different experimental conditions. In order to make our presentation of equilibrium data as homogeneous as possible, we will refer, when possible, to data obtained under equal, or very similar, experimental conditions. To help readers in the evaluation of the equilibrium data reported, we have included, when possible, all experimental conditions and the ligand protonation constants employed in the

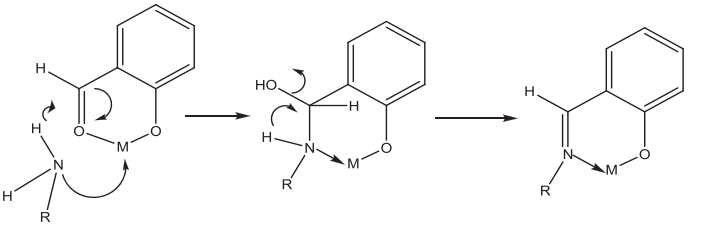

Scheme 2. Template synthesis of Schiff-base complexes.

determination of the stability constants of the complexes. There are two ways in which the enthalpy change accompanying a chemical process can be determined. One is to measure directly by a calorimeter the amount of heat involved in the reaction. In this case, there are instrumental limitations, at present, for the accurate determination of thermal effects that develop over very long times (days or weeks), as required by complexation reactions of macrocyclic polyamino-polycarboxylate ligands. The other problem consists of determining the equilibrium constants at various temperatures, and applying the van't Hoff isochore to derive the value of $\Delta H°$. Once $\Delta H°$ is known, the entropy term $\Delta S°$ can be obtained from the relationship $\Delta G° = \Delta H° - T\Delta S°$, the standard free energy change being related to the equilibrium constant by $\Delta G° = -RT \ln K$. Of these two methods, the second may lead to large uncertainties if not used with care. Since there is a logarithmic correlation between stability constants and $\Delta H°$, the propagation of the experimental errors in the determination of equilibrium constants on the enthalpy is exponential:

$$\delta(R\log K)/\delta(1/T) = -\Delta H^{\circ} \text{ and } \log K = -\Delta H^{\circ}/2.303RT + \text{const.}$$

Therefore, the temperature range explored should be as wide as possible and the equilibrium constants have to be of great accuracy.

2.6. *Determination of protonation constants*

Protonation constants are the equilibrium constants for interaction of the proton with charged or uncharged ligands depending on the availability of hydrogen ions in natural waters and biofluids. These parameters are used to predict the ionization state of the molecule with respect to pH. The determination of equilibrium constants is an important process for many branches of chemistry [27]. The major reasons for the determination of protonation constants can be summarized as follows:

- Protonation constants are important in preparative chemistry as well. If the protonation constants of a certain substance are known, it is possible to isolate it with a maximum yield by finding the pH range where the compound shows minimum ionization.
- Protonation of a newly synthesized compound can also give supportive information about its structure. If theoretically calculated protonation constants are in accord with experimental values, it is possible that the proposed structure could be correct.
- One can calculate the pH and the ratio of different forms of a certain substance by use of its protonation constants.
- Due to the fact that different forms of different substances have different UV spectra, by choosing a suitable pH value one can carry out spectrophotometric quantitative analyses. The choice of the pH value requires knowledge of the protonation constants.
- It is necessary that the protonation constants be known in order to prepare buffer solutions at different pH values [28]. There are various techniques such as conductometry, spectrophotometry, and potentiometry [29–31] that are used in the determination of protonation constants.
- In addition, for calculations of stability constants of complex formation of biologically active ligands with metal ions, their protonation constants are used [11].

Developments in the field of computation of equilibrium constants from experimental data were reviewed by Leggett [32] and Meloun *et al.* [33]. Since that time, many more programs have been published, mainly to use microcomputers for the computations. The most commonly used programs for solution equilibrium constant determination are PKPOT [34], PKAS [35], BEST [36], MINIQUAD [37], MINIQUAD-75 [38], SUPERQUAD [39], PSEQUAD [40], and HYPERQUAD [41]. All of these programs use least-square refinements to reduce the differences between calculated and experimental data to get the best model. The sum of the square of residuals between experimental and calculated values is normally very small, typically between 10^{-6} and 10^{-9}.

2.7. *Calculation of the stability constants*

Many computer programs are available for calculating stability constants of complexes in solution from experimental data. Most of these programs obtain the best-fit stability constants for a system by using the least-squares method, minimizing the difference between the calculated and observed pH values for all titration points. The core algorithm consists of computation by successive approximations of the pH_m values at each equilibrium point from an initial set of stability constants based on the equilibrium model. Each approximation results in adjustment of the equilibrium constants that are being refined in order to improve the fit between calculated and observed pH_m values.

2.8. *Hydrolysis of SBs*

SBs usually undergo partial hydrolysis at imine linkages $-C^{\delta+}=N^{\delta-}-$ and the mechanism of hydrolysis of imines is understood very well. At the imine bond, the positively charged carbon is attacked by water, which on subsequent release of protons breaks the imine linkage. The complete mechanism of the hydrolysis of an imine linkage is shown in scheme 3 [42].

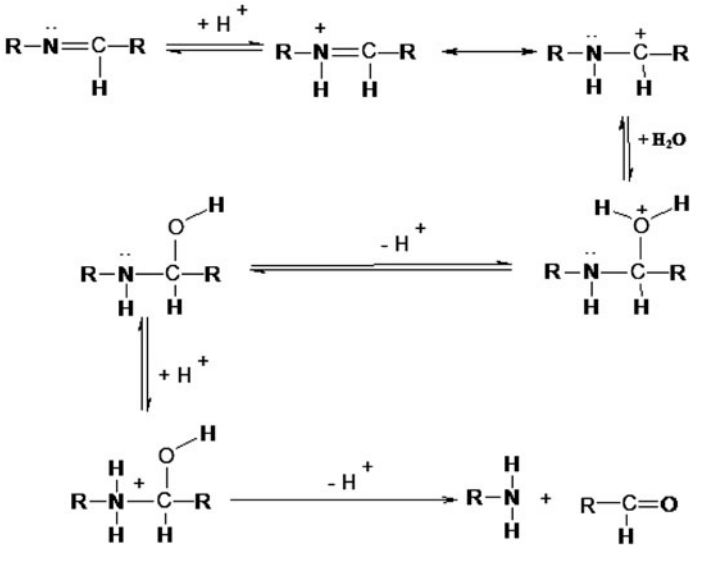

Scheme 3. Hydrolysis mechanism of an imine linkage.

A major difficulty in obtaining reliable values for protonation constants of most synthesized SBs, especially those derived from aromatic amines, is due to their low solubility and possible hydrolysis in aqueous solutions. Therefore, it is necessary to work at low concentrations and pH should be neither extremely low nor extremely high. Thus, the study of these SBs requires the use of an organic or aqueous-organic solvent which can dissolve these compounds and which furthermore presents compatibility with the standard glass electrode, such that the e.m.f. measurements can be carried out in a manner similar to when water is used. In this context, DMSO–water [43–48] as well as dioxane–water [49, 50] mixtures have been reported to be suitable solvents for potentiometric study of SB complexes. Other aqueous-organic solvents such as ethanol–water [51–53] and acetone–water [53] have also been used, although less extensively.

2.9. *Protonation and complex-formation equilibria of salicylaldehyde SBs and their derivatives*

2.9.1. Salicylaldehyde SBs derived from triethylenetetramine (Sal_2trien). SBs, especially those with a N_2O_2 donor set, resulting from condensation of aliphatic diamines such as ethylenediamine or derivatives with acetylacetone or salicylaldehyde, have been extensively studied [54]. The hexadentate Schiff-base (Sal_2trien) ligand (C1), where Sal = salicylaldehyde and trien = triethylenetetramine, has been synthesized by the reaction between salicylaldehyde and triethylenetetramine [55] as shown in scheme 4. Protonation constants of the Sal_2trien Schiff base and its complex-formation equilibria with Zn(II) were determined by potentiometric titration and the results are given in table 1.

Species distribution curves of Sal_2trien and ZnL show that more than 90% of LH_4 exists at pH below 4.0. LH_3 exists from pH 3.0 to 7.0 and its maximum population (30%) is located at pH 5.2. From pH 6.0 to 7.5, LH_2 is the dominant species (~80%). Species of LH and L are present at pH above 6.5 and 8.0, respectively. The ZnL complex is present at pH above 8.5 and increases with increasing pH.

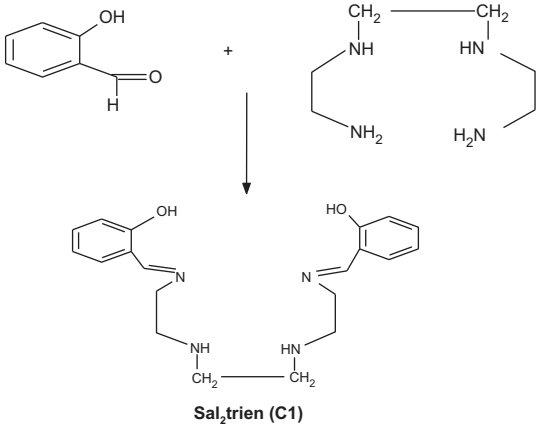

Scheme 4. Hexadentate Schiff base (Sal_2trien) (C1).

Table 1. Equilibrium constants for protonation and complex formation of salicylaldehyde SBs.

Reaction	log K	Method[a]	T°C	Medium	$\Delta H°$	$\Delta S°$	$\Delta G°$ [b]	Refs.
Sal_2trien (C1)								
$L^{2-} + H^+ \rightleftharpoons HL^-$	12.74	Pot.	25	0.1 M NaCl				[55]
$LH^- + H^+ \rightleftharpoons H_2L$	12.12	Pot.	25	0.1 M NaCl				[55]
$H_2L + H^+ \rightleftharpoons H_3L^+$	9.10	Pot.	25	0.1 M NaCl				[55]
$H_3L^+ + H^+ \rightleftharpoons H_4L^{2-}$	6.79	Pot.	25	0.1 M NaCl				[55]
$Zn^{2+} + L^{2-} \rightleftharpoons ZnL$	4.25	Pot.	25	0.1 M NaCl				[55]
2-((phenylimino)methyl)phenol (C2)								
$L^- + H^+ \rightleftharpoons LH$	7.60	Sp.	25					[56]
$L^- + H^+ \rightleftharpoons LH$	7.35	Pot.	25					[56]
$Cu^{2+} + L^- \rightleftharpoons CuL^+$	6.92	Pot.	25				−73.37	[56]
$Cu^{2+} + 2L^- \rightleftharpoons CuL$	5.94	Pot.						[56]
$Ni^{2+} + L^- \rightleftharpoons NiL$	6.81	Pot.	25				−69.77	[56]
$Ni^{2+} + 2L^- \rightleftharpoons NiL^+$	5.42	Pot.						[56]
$Fe^{3+} + 2L^- \rightleftharpoons FeL^{2+}$	6.60	Pot.	25				−66.75	[56]
$Fe^{3+} + L^- \rightleftharpoons FeL^+$	5.10	Pot.						[56]
$Cr^{3+} + L^- \rightleftharpoons CrL^{3+}$	5.97	Pot.	25				−58.02	[56]
$Cr^{3+} + 2L^- \rightleftharpoons CrL^+$	4.20	Pot.						[56]
$Mn^{2+} + L^- \rightleftharpoons MnL^+$	4.45	Pot.	25				−44.96	[56]
$Mn^{2+} + 2L^- \rightleftharpoons MnL$	3.43	Pot.						[56]
H_2sal-o-phen (H_2L) (C3)								
$L^{2-} + H^+ \rightleftharpoons LH^-$	10.94	Pot.	25	0.5 M $NaClO_4$				[44]
$LH^- + H^+ \rightleftharpoons H_2L$	9.39	Pot.	25	0.5 M $NaClO_4$				[44]
$H_2L + H^+ \rightleftharpoons H_3L^+$	3.46	Pot.	25	0.5 M $NaClO_4$				[44]
$Fe^{3+} + H^+ + \rightleftharpoons FeLH$	10.58	Pot.	25	0.5 M $NaClO_4$				[44]
$Fe^{3+} + L \rightleftharpoons FeL$	17.80	Pot.	25	0.5 M $NaClO_4$				[44]
$Ni^{2+} + H^+ + L \rightleftharpoons NiLH$	9.08	Pot.	25	0.5 M $NaClO_4$				[44]
$Ni^{2+} + L \rightleftharpoons NiL$	14.82	Pot.	25	0.5 M $NaClO_4$				[44]
$Co^{2+} + H^+ + L \rightleftharpoons CoLH$	9.81	Pot.	25	0.5 M $NaClO_4$				[44]
$Co^{2+} + L \rightleftharpoons CoL$	14.64	Pot.	25	0.5 M $NaClO_4$				[44]
$Zn^{2+} + H^+ + L \rightleftharpoons ZnLH$	7.07	Pot.	25	0.5 M $NaClO_4$				[44]
$Zn^{2+} + L \rightleftharpoons ZnL$	13.31	Pot.	25	0.5 M $NaClO_4$				[44]
$Mg^{2+} + H^+ + L \rightleftharpoons MgLH$	3.62	Pot.	25	0.5 M $NaClO_4$				[44]

(*Continued*)

Table 1. (*Continued*).

Reaction	log *K*	Method[a]	*T*°C	Medium	Δ*H*°	Δ*S*°	Δ*G*° [b]	Refs.
Sal_2trien (C1)								
$Mg^{2+} + L \rightleftharpoons MgL$	6.28	Pot.	25	0.5 M $NaClO_4$				[44]
$Ca^{2+} + H^+ + L \rightleftharpoons CaLH$	2.55	Pot.	25	0.5 M $NaClO_4$				[44]
$Ca^{2+} + L \rightleftharpoons CaL$	4.27	Pot.	25	0.5 M $NaClO_4$				[44]
H_2sal-4-Cl-o-phen (C4)								
$L^{2-} + H^+ \rightleftharpoons LH^-$	10.26	Pot.	25	0.5 M $NaClO_4$				[57]
$LH^- + H^+ \rightleftharpoons H_2L$	9.20	Pot.	25	0.5 M $NaClO_4$				[57]
$H_2L + H^+ \rightleftharpoons H_3L^+$	2.70	Pot.	25	0.5 M $NaClO_4$				[57]
$Co^{2+} + H^+ + L \rightleftharpoons CoLH$	9.13	Pot.	25	0.5 M $NaClO_4$				[57]
$Co^{2+} + L \rightleftharpoons CoL$	14.41	Pot.	25	0.5 M $NaClO_4$				[57]
$Zn^{2+} + H^+ + L \rightleftharpoons ZnLH$	6.36	Pot.	25	0.5 M $NaClO_4$				[57]
$Zn^{2+} + L \rightleftharpoons ZnL$	11.90	Pot.	25	0.5 M $NaClO_4$				[57]
$Mg^{2+} + H^+ + L \rightleftharpoons MgLH$	3.42	Pot.	25	0.5 M $NaClO_4$				[57]
$Mg^{2+} + L \rightleftharpoons MgL$	4.41	Pot.	25	0.5 M $NaClO_4$				[57]
$Ca^{2+} + H^+ + L \rightleftharpoons CaLH$	2.05	Pot.	25	0.5 M $NaClO_4$				[57]
$Ca^{2+} + L \rightleftharpoons CaL$	3.45	Pot.	25	0.5 M $NaClO_4$				[57]
3-F-H_2sal-o-phen (C5)								
$L^{2-} + H^+ \rightleftharpoons LH^-$	11.23	Pot.	25	0.1 M KCl				[49]
$LH^- + H^+ \rightleftharpoons H_2L$	8.41	Pot.	25	0.1 M KCl				[49]
$H_2L + H^+ \rightleftharpoons H_3L^+$	3.17	Pot.	25	0.1 M KCl				[49]
$Co^{2+} + H^+ + L \rightleftharpoons CoLH$	10.62	Pot.	25	0.1 M KCl				[49]
$Co^{2+} + L \rightleftharpoons CoL$	14.91	Pot.	25	0.1 M KCl				[49]
H_2sal-m-phen(C6)								
$L^{2-} + H^+ \rightleftharpoons LH^-$	10.49	Pot.	25	0.1 M $NaClO_4$				[46]
$LH^- + H^+ \rightleftharpoons H_2L$	9.30	Pot.	25	0.1 M $NaClO_4$				[46]
$H_2L + H^+ \rightleftharpoons H_3L^+$	3.70	Pot.	25	0.1 M $NaClO_4$				[46]
$Cu^{2+} + H^+ + L \rightleftharpoons MLH$	8.13	Pot.	25	0.1 M $NaClO_4$				[46]
$Cu^{2+} + L \rightleftharpoons ML$	13.0	Pot.	25	0.1 M $NaClO_4$				[46]
$2\ Cu^{2+} + 2L \rightleftharpoons Cu_2L_2$	30.20	Pot.	25	0.1 M $NaClO_4$				[46]
$2\ Cu^{2+} + L \rightleftharpoons Cu_2L$	16.47	Pot.	25	0.1 M $NaClO_4$				[46]
$Ni^{2+} + H^+ + L \rightleftharpoons NiLH$	5.51	Pot.	25	0.1 M $NaClO_4$				[46]
$Ni^{2+} + L \rightleftharpoons NiL$	7.45	Pot.	25	0.1 M $NaClO_4$				[46]
$Ni^{2+} + 2L \rightleftharpoons NiL_2$	11.16	Pot.	25	0.1 M $NaClO_4$				[46]
$2\ Ni^{2+} + 2L \rightleftharpoons Ni_2L_2$	18.04	Pot.	25	0.1 M $NaClO_4$				[46]
$2\ Ni^{2+} + L \rightleftharpoons Ni_2L$	11.69	Pot.	25	0.1 M $NaClO_4$				[46]

$Co^{2+} + H^+ + L \rightleftharpoons CoLH$	5.11	Pot.	25	0.1 M $NaClO_4$	[46]
$Co^{2+} + L \rightleftharpoons CoL$	7.13	Pot.	25	0.1 M $NaClO_4$	[46]
$Co^{2+} + 2L \rightleftharpoons CoL_2$	11.06	Pot.	25	0.1 M $NaClO_4$	[46]
$2Co^{2+} + L \rightleftharpoons Co_2L$	17.75	Pot.	25	0.1 M $NaClO_4$	[46]
$2Co^{2+} + L \rightleftharpoons Co_2L$	10.82	Pot.	25	0.1 M $NaClO_4$	[46]
$Zn^{2+} + H^+ + L \rightleftharpoons ZnLH$	4.69	Pot.	25	0.1 M $NaClO_4$	[46]
$Zn^{2+} + L \rightleftharpoons ZnL$	6.56	Pot.	25	0.1 M $NaClO_4$	[46]
$2Zn^{2+} + 2L \rightleftharpoons Zn_2L_2$	16.80	Pot.	25	0.1 M $NaClO_4$	[46]
$2\ Zn^{2+} + L \rightleftharpoons Zn_2L$	10.35	Pot.	25	0.1 M $NaClO_4$	[46]
H_2sal-2,4-toulene (C7)					
$L^{2-} + H^+ \rightleftharpoons LH$	10.61	Pot.	25	0.1 M $NaClO_4$	[46]
$LH^- + H^+ \rightleftharpoons H_2L$	9.43	Pot.	25	0.1 M $NaClO_4$	[46]
$H_2L + H^+ \rightleftharpoons H_3L^+$	3.96	Pot.	25	0.1 M $NaClO_4$	[46]
$Co^{2+} + H^+ + L \rightleftharpoons CoLH$	5.57	Pot.	25	0.1 M $NaClO_4$	[46]
$Co^{2+} + L \rightleftharpoons CoL$	7.85	Pot.	25	0.1 M $NaClO_4$	[46]
$Co^{2+} + 2L \rightleftharpoons CoL_2$	12.12	Pot.	25	0.1 M $NaClO_4$	[46]
$2Co^{2+} + L \rightleftharpoons Co_2L$	11.73	Pot.	25	0.1 M $NaClO_4$	[46]
$2Co^{2+} + 2\ L \rightleftharpoons Co_2L_2$	19.19	Pot.	25	0.1 M $NaClO_4$	[46]
$Cu^{2+} + H^+ + L \rightleftharpoons CuLH$	8.32	Pot.	25	0.1 M $NaClO_4$	[46]
$Cu^{2+} + L \rightleftharpoons CuL$	13.42	Pot.	25	0.1 M $NaClO_4$	[46]
$2Cu^{2+} + L \rightleftharpoons Cu_2L$	17.20	Pot.	25	0.1 M $NaClO_4$	[46]
$2Cu^{2+} + 2\ L \rightleftharpoons Cu_2L_2$	31.36	Pot.	25	0.1 M $NaClO_4$	[46]
$Zn^{2+} + H^+ + L \rightleftharpoons Zn\ LH$	5.27	Pot.	25	0.1 M $NaClO_4$	[46]
$Zn^{2+} + L \rightleftharpoons Zn\ L$	7.29	Pot.	25	0.1 M $NaClO_4$	[46]
$2\ Zn^{2+} + L \rightleftharpoons Zn_2L$	10.07	Pot.	25	0.1 M $NaClO_4$	[46]
$2\ Zn^{2+} + 2\ L \rightleftharpoons Zn_2L_2$	18.25	Pot.	25	0.1 M $NaClO_4$	[46]
$Ni^{2+} + H^+ + L \rightleftharpoons NiLH$	5.71	Pot.	25	0.1 M $NaClO_4$	[46]
$Ni^{2+} + L \rightleftharpoons Ni\ L$	7.84	Pot.	25	0.1 M $NaClO_4$	[46]
$Ni^{2+} + 2L \rightleftharpoons Ni\ L_2$	11.60	Pot.	25	0.1 M $NaClO_4$	[46]
$2\ Ni^{2+} + L \rightleftharpoons Ni_2L$	17.20	Pot.	25	0.1 M $NaClO_4$	[46]
$2\ Ni^{2+} + 2\ L \rightleftharpoons Ni_2L_2$	18.67	Pot.	25	0.1 M $NaClO_4$	[46]
H_2sal-2,6-toulene(C8)					
$L^{2-} + H^+ \rightleftharpoons LH^-$	10.72	Pot.	25	0.1 M $NaClO_4$	[46]
$LH^- + H^+ \rightleftharpoons H_2L$	9.42	Pot.	25	0.1 M $NaClO_4$	[46]
$H_2L + H^+ \rightleftharpoons H_3L^+$	3.80	Pot.	25	0.1 M $NaClO_4$	[46]
$Co^{2+} + H^+ + L \rightleftharpoons CoLH$	5.01	Pot.	25	0.1 M $NaClO_4$	[46]

(*Continued*)

Table 1. (*Continued*).

Reaction	log *K*	Method[a]	*T* °C	Medium	Δ*H*°	Δ*S*°	Δ*G*° [b]	Refs.
Sal_2trien (C1)								
$Co^{2+} + L \rightleftharpoons CoL$	6.90	Pot.	25	0.1 M $NaClO_4$				[46]
$Co^{2+} + 2L \rightleftharpoons CoL_2$	11.10	Pot.	25	0.1 M $NaClO_4$				[46]
$2Co^{2+} + L \rightleftharpoons Co_2L$	10.74	Pot.	25	0.1 M $NaClO_4$				[46]
$2Co^{2+} + 2L \rightleftharpoons Co_2L_2$	16.80	Pot.	25	0.1 M $NaClO_4$				[46]
$Cu^{2+} + H^+ + L \rightleftharpoons CuLH$	8.17	Pot.	25	0.1 M $NaClO_4$				[46]
$Cu^{2+} + L \rightleftharpoons CuL$	12.66	Pot.	25	0.1 M $NaClO_4$				[46]
$2Cu^{2+} + L \rightleftharpoons Cu_2L$	16.58	Pot.	25	0.1 M $NaClO_4$				[46]
$2Cu^{2+} + 2\,L \rightleftharpoons Cu_2L_2$	28.14	Pot.	25	0.1 M $NaClO_4$				[46]
$Zn^{2+} + H^+ + L \rightleftharpoons Zn\,LH$	4.46	Pot.	25	0.1 M $NaClO_4$				[46]
$Zn^{2+} + L \rightleftharpoons Zn\,L$	7.01	Pot.	25	0.1 M $NaClO_4$				[46]
$2\,Zn^{2+} + L \rightleftharpoons Zn_2L$	9.80	Pot.	25	0.1 M $NaClO_4$				[46]
$2\,Zn^{2+} + 2\,L \rightleftharpoons Zn_2L_2$	16.80	Pot.	25	0.1 M $NaClO_4$				[46]
$Ni^{2+} + H^+ + L \rightleftharpoons NiLH$	5.47	Pot.	25	0.1 M $NaClO_4$				[46]
$Ni^{2+} + L \rightleftharpoons Ni\,L$	6.90	Pot.	25	0.1 M $NaClO_4$				[46]
$Ni^{2+} + 2L \rightleftharpoons Ni\,L_2$	11.10	Pot.	25	0.1 M $NaClO_4$				[46]
$2\,Ni^{2+} + L \rightleftharpoons Ni_2L$	11.67	Pot.	25	0.1 M $NaClO_4$				[46]
$2\,Ni^{2+} + 2\,L \rightleftharpoons Ni_2L_2$	17.47	Pot.	25	0.1 M $NaClO_4$				[46]
2-Aminomethylthiophene and 4-bromosalicylaldehyde (ATS) (C9)								
$L^- + H^+ \rightleftharpoons LH$	9.96	Pot.	25	0.1 M $NaNO_3$	−59.86	−57.62	−42.11	[10]
$L^- + H^+ \rightleftharpoons LH$	9.17	Pot.	35	0.1 M $NaNO_3$				[10]
$L^- + H^+ \rightleftharpoons LH$	8.38	Pot.	45	0.1 M $NaNO_3$				[10]
$LH + H^+ \rightleftharpoons LH_2^+$	7.47	Pot.	25	0.1 M $NaNO_3$	−143.29	−289.64	−54.08	[10]
$LH + H^+ \rightleftharpoons LH_2^+$	7.14	Pot.	35	0.1 M $NaNO_3$				[10]
$LH + H^+ \rightleftharpoons LH_2^+$	6.81	Pot.	45	0.1 M $NaNO_3$				[10]
$Mn^{2+} + L^- \rightleftharpoons MnL^+$	5.28	Pot.	25	0.1 M $NaNO_3$	−126.97	−324.55	−27.01	[10]
$Mn^{2+} + L^- \rightleftharpoons MnL^+$	4.58	Pot.	35	0.1 M $NaNO_3$				[10]
$Mn^{2+} + L^- \rightleftharpoons MnL^+$	3.88	Pot.	45	0.1 M $NaNO_3$				[10]
$Co^{2+} + L^- \rightleftharpoons CoL^+$	6.36	Pot.	25	0.1 M $NaNO_3$	−167.81	−441.08	−31.96	[10]
$Co^{2+} + L^- \rightleftharpoons CoL^+$	5.42	Pot.	35	0.1 M $NaNO_3$				[10]
$Co^{2+} + L^- \rightleftharpoons CoL^+$	4.51	Pot.	45	0.1 M $NaNO_3$				[10]
$Ni^{2+} + L^- \rightleftharpoons NiL^+$	6.65	Pot.	25	0.1 M $NaNO_3$	−176.88	−467.28	−32.97	[10]
$Ni^{2+} + L^- \rightleftharpoons NiL^+$	5.59	Pot.	35	0.1 M $NaNO_3$				[10]
$Ni^{2+} + L^- \rightleftharpoons NiL^+$	4.63	Pot.	45	0.1 M $NaNO_3$				[10]

$Cu^{2+} + L^- \rightleftharpoons CuL^+$	9.41	Pot.	25	0.1 M $NaNO_3$	−185.02	−440.05	−49.48	[10]
$Cu^{2+} + L^- \rightleftharpoons CuL^+$	8.39	Pot.	35	0.1 M $NaNO_3$				[10]
$Cu^{2+} + L^- \rightleftharpoons CuL^+$	7.37	Pot.	45	0.1 M $NaNO_3$				[10]
$Zn^{2+} + L^- \rightleftharpoons ZnL^+$	6.07	Pot.	25	0.1 M $NaNO_3$	−148.74	−382.40	−30.96	[10]
$Zn^{2+} + L^- \rightleftharpoons ZnL^+$	5.25	Pot.	35	0.1 M $NaNO_3$				[10]
$Zn^{2+} + L^- \rightleftharpoons ZnL^+$	4.43	Pot.	45	0.1 M $NaNO_3$				[10]
2-((pyridyl-2-imino)methyl)phenol (SAPy)(C10)								
$L^- + H^+ \rightleftharpoons LH$	9.25	Pot.	25	0.1 M $NaNO_3$				[66]
$L^- + H^+ \rightleftharpoons LH$	9.02	Pot.	50	0.1 M $NaNO_3$				[66]
$LH + H^+ \rightleftharpoons LH_2^+$	6.41	Pot.	25	0.1 M $NaNO_3$				[66]
$LH + H^+ \rightleftharpoons LH_2^+$	6.30	Pot.	50	0.1 M $NaNO_3$				[66]
$Cu^{2+} + L^- \rightleftharpoons CuL^+$	6.86	Pot.	25	0.1 M $NaNO_3$				[56]
$Cu^{2+} + 2L^- \rightleftharpoons CuL$	6.10	Pot.	25	0.1 M $NaNO_3$				[56]
$Ni^{2+} + L^- \rightleftharpoons NiL$	6.82	Pot.	25	0.1 M $NaNO_3$				[56]
$Ni^{2+} + 2L^- \rightleftharpoons NiL^+$	5.52	Pot.	25	0.1 M $NaNO_3$				[56]
$Fe^{3+} + 2L^- \rightleftharpoons FeL^{2+}$	6.62	Pot.	25	0.1 M $NaNO_3$				[56]
$Fe^{3+} + L^- \rightleftharpoons FeL^+$	5.21	Pot.	25	0.1 M $NaNO_3$				[56]
$Cr^{3+} + L^- \rightleftharpoons CrL^{3+}$	6.19	Pot.	25	0.1 M $NaNO_3$				[56]
$Cr^{3+} + 2L^- \rightleftharpoons CrL^+$	4.93	Pot.	25	0.1 M $NaNO_3$				[56]
$Mn^{2+} + L^- \rightleftharpoons MnL^+$	5.02	Pot.	25	0.1 M $NaNO_3$				[56]
$Mn^{2+} + 2L^- \rightleftharpoons MnL$	3.81	Pot.	25	0.1 M $NaNO_3$				[56]
$La^{3+} + L^- \rightleftharpoons LaL^{2+}$	4.69	Pot.	25	0.1 M $NaNO_3$				[66]
$La^{3+} + L^- \rightleftharpoons LaL^{2+}$	4.31	Pot.	50	0.1 M $NaNO_3$				[66]
$LaL^{2+} + L^- \rightleftharpoons LaL_2^+$	3.52	Pot.	25	0.1 M $NaNO_3$				[66]
$LaL^{2+} + L^- \rightleftharpoons LaL_2^+$	3.24	Pot.	50	0.1 M $NaNO_3$				[66]
$LaL^{2+} + L^- \rightleftharpoons LaL_3$	2.65	Pot.	25	0.1 M $NaNO_3$				[66]
$LaL^{2+} + L^- \rightleftharpoons LaL_3$	2.40	Pot.	50	0.1 M $NaNO_3$				[66]
$Pr^{3+} + L^- \rightleftharpoons PrL^{2+}$	5.15	Pot.	25	0.1 M $NaNO_3$				[66]
$Pr^{3+} + L^- \rightleftharpoons PrL^{2+}$	4.74	Pot.	50	0.1 M $NaNO_3$				[66]
$PrL^{2+} + L^- \rightleftharpoons PrL_2^+$	3.52	Pot.	25	0.1 M $NaNO_3$				[66]
$PrL^{2+} + L^- \rightleftharpoons PrL_2^+$	4.02	Pot.	50	0.1 M $NaNO_3$				[66]
$PrL^{2+} + L^- \rightleftharpoons PrL_3$	2.97	Pot.	25	0.1 M $NaNO_3$				[66]
$PrL^{2+} + L^- \rightleftharpoons PrL_3$	2.74	Pot.	50	0.1 M $NaNO_3$				[66]
$Nd^{3+} + L^- \rightleftharpoons NdL^{2+}$	5.32	Pot.	25	0.1 M $NaNO_3$				[66]
$Nd^{3+} + L^- \rightleftharpoons NdL^{2+}$	4.90	Pot.	50	0.1 M $NaNO_3$				[66]
$NdL^{2+} + L^- \rightleftharpoons NdL_2^+$	4.15	Pot.	25	0.1 M $NaNO_3$				[66]
$NdL^{2+} + L^- \rightleftharpoons NdL_2^+$	3.81	Pot.	50	0.1 M $NaNO_3$				[66]

(*Continued*)

Table 1. (*Continued*).

Reaction	log *K*	Method[a]	*T* °C	Medium	Δ*H*°	Δ*S*°	Δ*G*° [b]	Refs.
Sal_2trien (C1)								
$NdL^{2+} + L^- \rightleftharpoons NdL_3$	3.08	Pot.	25	0.1 M $NaNO_3$				[66]
$NdL^{2+} + L^- \rightleftharpoons NdL_3$	2.84	Pot.	50	0.1 M $NaNO_3$				[66]
$Eu^{3+} + L^- \rightleftharpoons EuL^{2+}$	6.15	Pot.	25	0.1 M $NaNO_3$				[66]
$Eu^{3+} + L^- \rightleftharpoons EuL^{2+}$	5.69	Pot.	50	0.1 M $NaNO_3$				[66]
$EuL^{2+} + L^- \rightleftharpoons EuL_2^+$	4.31	Pot.	25	0.1 M $NaNO_3$				[66]
$EuL^{2+} + L^- \rightleftharpoons EuL_2^+$	3.97	Pot.	50	0.1 M $NaNO_3$				[66]
$EuL^{2+} + L^- \rightleftharpoons EuL_3$	3.21	Pot.	25	0.1 M $NaNO_3$				[66]
$EuL^{2+} + L^- \rightleftharpoons EuL_3$	2.97	Pot.	50	0.1 M $NaNO_3$				[66]
$Ho^{3+} + L^- \rightleftharpoons HoL^{2+}$	6.25	Pot.	25	0.1 M $NaNO_3$				[66]
$Ho^{3+} + L^- \rightleftharpoons HoL^{2+}$	5.79	Pot.	50	0.1 M $NaNO_3$				[66]
$HoL^{2+} + L^- \rightleftharpoons HoL_2^+$	4.57	Pot.	25	0.1 M $NaNO_3$				[66]
$HoL^{2+} + L^- \rightleftharpoons HoL_2^+$	4.22	Pot.	50	0.1 M $NaNO_3$				[66]
$HoL^{2+} + L^- \rightleftharpoons HoL_3$	3.31	Pot.	25	0.1 M $NaNO_3$				[66]
$HoL^{2+} + L^- \rightleftharpoons HoL_3$	3.05	Pot.	50	0.1 M $NaNO_3$				[66]
$Yb^{3+} + L^- \rightleftharpoons YbL^{2+}$	6.52	Pot.	25	0.1 M $NaNO_3$				[66]
$Yb^{3+} + L^- \rightleftharpoons YbL^{2+}$	6.04	Pot.	50	0.1 M $NaNO_3$				[66]
$YbL^{2+} + L^- \rightleftharpoons YbL_2^+$	4.75	Pot.	25	0.1 M $NaNO_3$				[66]
$YbL^{2+} + L^- \rightleftharpoons YbL_2^+$	4.38	Pot.	50	0.1 M $NaNO_3$				[66]
$YbL^{2+} + L^- \rightleftharpoons YbL_3$	3.57	Pot.	25	0.1 M $NaNO_3$				[66]
$YbL^{2+} + L^- \rightleftharpoons YbL_3$	3.29	Pot.	50	0.1 M $NaNO_3$				[66]
SAPyMe (C11)								
$L^- + H^+ \rightleftharpoons LH$	9.56	Pot.	25	0.1 M $NaNO_3$				[66]
$L^- + H^+ \rightleftharpoons LH$	9.47	Pot.	50	0.1 M $NaNO_3$				[66]
$LH + H^+ \rightleftharpoons LH_2^+$	7.09	Pot.	25	0.1 M $NaNO_3$				[66]
$LH + H^+ \rightleftharpoons LH_2^+$	6.54	Pot.	50	0.1 M $NaNO_3$				[66]
$La^{3+} + L^- \rightleftharpoons LaL^{2+}$	6.37	Pot.	25	0.1 M $NaNO_3$				[66]
$La^{3+} + L^- \rightleftharpoons LaL^{2+}$	5.85	Pot.	50	0.1 M $NaNO_3$				[66]
$LaL^{2+} + L^- \rightleftharpoons LaL_2^+$	4.06	Pot.	25	0.1 M $NaNO_3$				[66]
$LaL^{2+} + L^- \rightleftharpoons LaL_2^+$	4.02	Pot.	50	0.1 M $NaNO_3$				[66]
$LaL^{2+} + L^- \rightleftharpoons LaL_3$	4.03	Pot.	25	0.1 M $NaNO_3$				[66]
$LaL^{2+} + L^- \rightleftharpoons LaL_3$	3.73	Pot.	50	0.1 M $NaNO_3$				[66]
$Pr^{3+} + L^- \rightleftharpoons PrL^{2+}$	7.14	Pot.	25	0.1 M $NaNO_3$				[66]
$Pr^{3+} + L^- \rightleftharpoons PrL^{2+}$	6.57	Pot.	50	0.1 M $NaNO_3$				[66]
$PrL^{2+} + L^- \rightleftharpoons PrL_2^+$	4.92	Pot.	25	0.1 M $NaNO_3$				[66]

$PrL^{2+} + L^{-} \rightleftharpoons PrL_2^{+}$	4.54	Pot.	50	0.1 M $NaNO_3$	[66]
$PrL^{2+} + L^{-} \rightleftharpoons PrL_3$	4.40	Pot.	25	0.1 M $NaNO_3$	[66]
$PrL^{2+} + L^{-} \rightleftharpoons PrL_3$	4.06	Pot.	50	0.1 M $NaNO_3$	[66]
$Nd^{3+} + L^{-} \rightleftharpoons NdL^{2+}$	7.22	Pot.	25	0.1 M $NaNO_3$	[66]
$Nd^{3+} + L^{-} \rightleftharpoons NdL^{2+}$	6.69	Pot.	50	0.1 M $NaNO_3$	[66]
$NdL^{2+} + L^{-} \rightleftharpoons NdL_2^{+}$	5.08	Pot.	25	0.1 M $NaNO_3$	[66]
$NdL^{2+} + L^{-} \rightleftharpoons NdL_2^{+}$	4.69	Pot.	50	0.1 M $NaNO_3$	[66]
$NdL^{2+} + L^{-} \rightleftharpoons NdL_3$	4.51	Pot.	25	0.1 M $NaNO_3$	[66]
$NdL^{2+} + L^{-} \rightleftharpoons NdL_3$	4.16	Pot.	50	0.1 M $NaNO_3$	[66]
$Eu^{3+} + L^{-} \rightleftharpoons EuL^{2+}$	7.57	Pot.	25	0.1 M $NaNO_3$	[66]
$Eu^{3+} + L^{-} \rightleftharpoons EuL^{2+}$	7.00	Pot.	50	0.1 M $NaNO_3$	[66]
$EuL^{2+} + L^{-} \rightleftharpoons EuL_2^{+}$	5.20	Pot.	25	0.1 M $NaNO_3$	[66]
$EuL^{2+} + L^{-} \rightleftharpoons EuL_2^{+}$	4.80	Pot.	50	0.1 M $NaNO_3$	[66]
$EuL^{2+} + L^{-} \rightleftharpoons EuL_3$	4.72	Pot.	25	0.1 M $NaNO_3$	[66]
$EuL^{2+} + L^{-} \rightleftharpoons EuL_3$	4.35	Pot.	50	0.1 M $NaNO_3$	[66]
$Ho^{3+} + L^{-} \rightleftharpoons HoL^{2+}$	7.82	Pot.	25	0.1 M $NaNO_3$	[66]
$Ho^{3+} + L^{-} \rightleftharpoons HoL^{2+}$	7.24	Pot.	50	0.1 M $NaNO_3$	[66]
$HoL^{2+} + L^{-} \rightleftharpoons HoL_2^{+}$	5.42	Pot.	25	0.1 M $NaNO_3$	[66]
$HoL^{2+} + L^{-} \rightleftharpoons HoL_2^{+}$	5.00	Pot.	50	0.1 M $NaNO_3$	[66]
$HoL^{2+} + L^{-} \rightleftharpoons HoL_3$	4.81	Pot.	25	0.1 M $NaNO_3$	[66]
$HoL^{2+} + L^{-} \rightleftharpoons HoL_3$	4.44	Pot.	50	0.1 M $NaNO_3$	[66]
$Yb^{3+} + L^{-} \rightleftharpoons YbL^{2+}$	8.03	Pot.	25	0.1 M $NaNO_3$	[66]
$Yb^{3+} + L^{-} \rightleftharpoons YbL^{2+}$	7.44	Pot.	50	0.1 M $NaNO_3$	[66]
$YbL^{2+} + L^{-} \rightleftharpoons YbL_2^{+}$	5.61	Pot.	25	0.1 M $NaNO_3$	[66]
$YbL^{2+} + L^{-} \rightleftharpoons YbL_2^{+}$	5.15	Pot.	50	0.1 M $NaNO_3$	[66]
$YbL^{2+} + L^{-} \rightleftharpoons YbL_3$	4.94	Pot.	25	0.1 M $NaNO_3$	[66]
$YbL^{2+} + L^{-} \rightleftharpoons YbL_3$	4.54	Pot.	50	0.1 M $NaNO_3$	[66]
SAPyCl (C12)					
$L^{-} + H^{+} \rightleftharpoons LH$	8.98	Pot.	25	0.1 M $NaNO_3$	[66]
$L^{-} + H^{+} \rightleftharpoons LH$	8.90	Pot.	50	0.1 M $NaNO_3$	[66]
$LH + H^{+} \rightleftharpoons LH_2^{+}$	4.16	Pot.	25	0.1 M $NaNO_3$	[66]
$LH + H^{+} \rightleftharpoons LH_2^{+}$	3.69	Pot.	50	0.1 M $NaNO_3$	[66]
$La^{3+} + L^{-} \rightleftharpoons LaL^{2+}$	3.76	Pot.	25	0.1 M $NaNO_3$	[66]
$La^{3+} + L^{-} \rightleftharpoons LaL^{2+}$	3.45	Pot.	50	0.1 M $NaNO_3$	[66]
$LaL^{2+} + L^{-} \rightleftharpoons LaL_2^{+}$	3.16	Pot.	25	0.1 M $NaNO_3$	[66]
$LaL^{2+} + L^{-} \rightleftharpoons LaL_2^{+}$	2.91	Pot.	50	0.1 M $NaNO_3$	[66]

(*Continued*)

Table 1. (*Continued*).

Sal_2trien (C1)

Reaction	log *K*	Method[a]	*T* °C	Medium	Δ*H*°	Δ*S*°	Δ*G*° [b]	Refs.
$Pr^{3+} + L^- \rightleftharpoons PrL^{2+}$	4.26	Pot.	25	0.1 M $NaNO_3$				[66]
$Pr^{3+} + L^- \rightleftharpoons PrL^{2+}$	3.92	Pot.	50	0.1 M $NaNO_3$				[66]
$PrL^{2+} + L^- \rightleftharpoons PrL_2^{+}$	3.23	Pot.	25	0.1 M $NaNO_3$				[66]
$PrL^{2+} + L^- \rightleftharpoons PrL_2^{+}$	2.97	Pot.	50	0.1 M $NaNO_3$				[66]
$Nd^{3+} + L^- \rightleftharpoons NdL^{2+}$	4.42	Pot.	25	0.1 M $NaNO_3$				[66]
$Nd^{3+} + L^- \rightleftharpoons NdL^{2+}$	4.07	Pot.	50	0.1 M $NaNO_3$				[66]
$NdL^{2+} + L^- \rightleftharpoons NdL_2^{+}$	3.25	Pot.	25	0.1 M $NaNO_3$				[66]
$NdL^{2+} + L^- \rightleftharpoons NdL_2^{+}$	3.00	Pot.	50	0.1 M $NaNO_3$				[66]
$Eu^{3+} + L^- \rightleftharpoons EuL^{2+}$	4.95	Pot.	25	0.1 M $NaNO_3$				[66]
$Eu^{3+} + L^- \rightleftharpoons EuL^{2+}$	4.58	Pot.	50	0.1 M $NaNO_3$				[66]
$EuL^{2+} + L^- \rightleftharpoons EuL_2^{+}$	3.29	Pot.	25	0.1 M $NaNO_3$				[66]
$EuL^{2+} + L^- \rightleftharpoons EuL_2^{+}$	3.03	Pot.	50	0.1 M $NaNO_3$				[66]
$Ho^{3+} + L^- \rightleftharpoons HoL^{2+}$	5.28	Pot.	25	0.1 M $NaNO_3$				[66]
$Ho^{3+} + L^- \rightleftharpoons HoL^{2+}$	4.89	Pot.	50	0.1 M $NaNO_3$				[66]
$HoL^{2+} + L^- \rightleftharpoons HoL_2^{+}$	3.33	Pot.	25	0.1 M $NaNO_3$				[66]
$HoL^{2+} + L^- \rightleftharpoons HoL_2^{+}$	3.06	Pot.	50	0.1 M $NaNO_3$				[66]
$Yb^{3+} + L^- \rightleftharpoons YbL^{2+}$	5.35	Pot.	25	0.1 M $NaNO_3$				[66]
$Yb^{3+} + L^- \rightleftharpoons YbL^{2+}$	4.96	Pot.	50	0.1 M $NaNO_3$				[66]
$YbL^{2+} + L^- \rightleftharpoons YbL_2^{+}$	3.35	Pot.	25	0.1 M $NaNO_3$				[66]
$YbL^{2+} + L^- \rightleftharpoons YbL_2^{+}$	3.09	Pot.	50	0.1 M $NaNO_3$				[66]
2-(2-pyridyliminomethyl)phenol (C13)								
$L^- + H^+ \rightleftharpoons LH$	8.82	Sp.	25					[67]
$LH + H^+ \rightleftharpoons LH_2^{+}$	6.92	Sp.	25					[67]
$L^- + H^+ \rightleftharpoons LH$	9.77	Pot.	25					[70]
$LH + H^+ \rightleftharpoons LH_2^{+}$	6.37	Pot.	25					[70]
$L^- + H^+ \rightleftharpoons LH$	9.30	Sp.	25					[71]
$LH + H^+ \rightleftharpoons LH_2^{+}$	7.0	Sp.	25					[71]
2-(2-amino-3-pyridyliminomethyl)phenol (C14)								
$L^- + H^+ \rightleftharpoons LH$	10.01	Sp.	25					[67]
$LH + H^+ \rightleftharpoons LH_2^{+}$	5.92	Sp.	25					[67]
$LH_2^{+} + H^+ \rightleftharpoons LH_3^{2+}$	4.12	Sp.	25					[67]
N,N'-bis(salicylidene)-2,3-pyridinediamine (C15)								
$L^{2-} + H^+ \rightleftharpoons LH^-$	9.71	Sp.	25					[67]
$LH^- + H^+ \rightleftharpoons LH_2$	6.90	Sp.	25					[67]

$LH_2 + H^+ \rightleftharpoons LH_3^+$	4.40	Sp.	25					[67]
N,N′-bis(sakylidene)-2,6-pyridinediamine (C16)								
$L^{2-} + H^+ \rightleftharpoons LH^-$	8.75	Sp.	25					[67]
$LH^- + H^+ \rightleftharpoons LH_2$	7.09	Sp.	25					[67]
2-((pyrimidin-2-ylimino)methyl)phenol (C17)								
$L^- + H^+ \rightleftharpoons LH$	8.40	Sp.	25					[73]
$L^- + H^+ \rightleftharpoons LH$	8.55	Pot.	25					[73]
$Cu^{2+} + L^- \rightleftharpoons CuL^+$	7.66	Pot.	25					[73]
$Cu^{2+} + 2L^- \rightleftharpoons CuL$	6.62	Pot.	25					[73]
$Ni^{2+} + L^- \rightleftharpoons NiL$	7.88	Pot.	25					[73]
$Ni^{2+} + 2L^- \rightleftharpoons NiL^+$	6.09	Pot.	25					[73]
$Fe^{3+} + 2L^- \rightleftharpoons FeL^{2+}$	7.14	Pot.	25					[73]
$Fe^{3+} + L^- \rightleftharpoons FeL^+$	6.12	Pot.	25					[73]
$Cr^{3+} + L^- \rightleftharpoons CrL^{3+}$	6.44	Pot.	25					[73]
$Cr^{3+} + 2L^- \rightleftharpoons CrL^+$	5.35	Pot.	25					[73]
$Mn^{2+} + L^- \rightleftharpoons MnL^+$	5.19	Pot.	25					[73]
$Mn^{2+} + 2L^- \rightleftharpoons MnL$	3.78	Pot.	25					[73]
4-hydroxysalicylidene-2-amino pyrimidine (H_2sap) (C18)								
$L^{2-} + H^+ \rightleftharpoons LH^-$	10.20	pH	20	0.04 M KNO_3				[74]
$L^{2-} + H^+ \rightleftharpoons LH^-$	9.94	pH	30	0.04 M KNO_3				[74]
$L^{2-} + H^+ \rightleftharpoons LH^-$	9.71	pH	40	0.04 M KNO_3				[74]
$LH^- + H^+ \rightleftharpoons LH_2$	8.50	pH	20	0.04 M KNO_3				[74]
$LH^- + H^+ \rightleftharpoons LH_2$	8.32	pH	30	0.04 M KNO_3				[74]
$LH^- + H^+ \rightleftharpoons LH_2$	8.12	pH	40	0.04 M KNO_3				[74]
$Co^{2+} + L^{2-} \rightleftharpoons CoL$	4.0	pH	20	0.04 M KNO_3	114.9	110.9	−38.4	[74]
$Co^{2+} + L^{2-} \rightleftharpoons CoL$	4.90	pH	30	0.04 M KNO_3				[74]
$Co^{2+} + L^{2-} \rightleftharpoons CoL$	5.55	pH	40	0.04 M KNO_3				[74]
$Co^{2+} + 2\,L^{2-} \rightleftharpoons CoL_2^{2-}$	3.81	pH	20	0.04 M KNO_3	102.1	101.5	−25.0	[74]
$Co^{2+} + 2\,L^{2-} \rightleftharpoons CoL_2^{2-}$	4.30	pH	30	0.04 M KNO_3				[74]
$Co^{2+} + 2\,L^{2-} \rightleftharpoons CoL_2^{2-}$	5.16	pH	40	0.04 M KNO_3				[74]
$Ni^{2+} + L^{2-} \rightleftharpoons NiL$	4.44	pH	20	0.04 M KNO_3	175.4	132.3	−31.1	[74]
$Ni^{2+} + L^{2-} \rightleftharpoons NiL$	5.36	pH	30	0.04 M KNO_3				[74]
$Ni^{2+} + L^{2-} \rightleftharpoons NiL$	6.08	pH	40	0.04 M KNO_3				[74]
$Ni^{2+} + 2\,L^{2-} \rightleftharpoons NiL_2^{2-}$	3.87	pH	20	0.04 M KNO_3	104.0	101.5	−25.8	[74]
$Ni^{2+} + 2\,L^{2-} \rightleftharpoons NiL_2^{2-}$	4.55	pH	30	0.04 M KNO_3				[74]
$Ni^{2+} + 2\,L^{2-} \rightleftharpoons NiL_2^{2-}$	5.29	pH	40	0.04 M KNO_3				[74]
$Cu^{2+} + L^{2-} \rightleftharpoons CuL$	5.53	pH	20	0.04 M KNO_3	74.7	128.3	−35.5	[74]

(*Continued*)

Table 1. (*Continued*).

Reaction	log *K*	Method[a]	*T* °C	Medium	Δ*H*°	Δ*S*°	Δ*G*° [b]	Refs.
Sal_2trien (C1)								
$Cu^{2+} + L^{2-} \rightleftharpoons CuL$	6.11	pH	30	0.04 M KNO_3				[74]
$Cu^{2+} + L^{2-} \rightleftharpoons CuL$	6.55	pH	40	0.04 M KNO_3				[74]
$Cu^{2+} + 2\ L^{2-} \rightleftharpoons CuL_2^{2-}$	4.12	pH	20	0.04 M KNO_3	89.2	103.8	−26.3	[74]
$Cu^{2+} + 2\ L^{2-} \rightleftharpoons CuL_2^{2-}$	4.55	pH	30	0.04 M KNO_3				[74]
$Cu^{2+} + 2\ L^{2-} \rightleftharpoons CuL_2^{2-}$	5.29	pH	40	0.04 M KNO_3				[74]
$Pd^{2+} + L^{2-} \rightleftharpoons PdL$	6.37	pH	20	0.04 M KNO_3	−75.7	91.9	−32.6	[74]
$Pd^{2+} + L^{2-} \rightleftharpoons PdL$	5.65	pH	30	0.04 M KNO_3				[74]
$Pd^{2+} + L^{2-} \rightleftharpoons PdL$	5.10	pH	40	0.04 M KNO_3				[74]
$Pd^{2+} + 2\ L^{2-} \rightleftharpoons PdL_2^{2-}$	5.18	pH	20	0.04 M KNO_3	−76.6	74.7	−25.7	[74]
$Pd^{2+} + 2\ L^{2-} \rightleftharpoons PdL_2^{2-}$	4.45	pH	30	0.04 M KNO_3				[74]
$Pd^{2+} + 2\ L^{2-} \rightleftharpoons PdL_2^{2-}$	4.20	pH	40	0.04 M KNO_3				[74]
$Ag^{+} + L^{2-} \rightleftharpoons AgL^{+}$	7.16	pH	20	0.04 M KNO_3	−132.5	95.7	−35.8	[74]
$Ag^{+} + L^{2-} \rightleftharpoons AgL^{+}$	6.15	pH	30	0.04 M KNO_3				[74]
$Ag^{+} + L^{2-} \rightleftharpoons AgL^{-}$	5.30	pH	40	0.04 M KNO_3				[74]
$Ag^{+} + 2\ L^{2-} \rightleftharpoons AgL_2^{3-}$	6.65	pH	20	0.04 M KNO_3	−134.0	86.2	−38.1	[74]
$Ag^{+} + 2\ L^{2-} \rightleftharpoons AgL_2^{3-}$	5.55	pH	30	0.04 M KNO_3				[74]
$Ag^{+} + 2\ L^{2-} \rightleftharpoons AgL_2^{3-}$	4.90	pH	40	0.04 M KNO_3				[74]
(2-((2-phthalazin-1-yl)hydrazono)methyl)phenol) (SAH) (C19)								
$L^{-} + H^{+} \rightleftharpoons HL$	11.11	Pot.	20	0.1 M $NaNO_3$	−94.03	−108.04	−61.83	[7]
$L^{-} + H^{+} \rightleftharpoons HL$	10.87	Pot.	25	0.1 M $NaNO_3$				[7]
$L^{-} + H^{+} \rightleftharpoons HL$	10.52	Pot.	30	0.1 M $NaNO_3$				[7]
$L^{-} + H^{+} \rightleftharpoons HL$	10.32	Pot.	35	0.1 M $NaNO_3$				[7]
$HL + H^{+} \rightleftharpoons H_2L^{+}$	4.35	Pot.	20	0.1 M $NaNO_3$	−44.23	−67.58	−24.09	[7]
$HL + H^{+} \rightleftharpoons H_2L^{+}$	4.23	Pot.	25	0.1 M $NaNO_3$				[7]
$HL + H^{+} \rightleftharpoons H_2L^{+}$	4.09	Pot.	30	0.1 M $NaNO_3$				[7]
$HL + H^{+} \rightleftharpoons H_2L^{+}$	3.97	Pot.	35	0.1 M $NaNO_3$				[7]
$Mn^{2+} + L^{-} \rightleftharpoons MnL^{+}$	9.20	Pot.	20	0.1 M $NaNO_3$	−375.04	−1103.2	−46.26	[7]
$Mn^{2+} + L^{-} \rightleftharpoons MnL^{+}$	8.20	Pot.	25	0.1 M $NaNO_3$				[7]
$Mn^{2+} + L^{-} \rightleftharpoons MnL^{+}$	6.89	Pot.	30	0.1 M $NaNO_3$				[7]
$Mn^{2+} + L^{-} \rightleftharpoons MnL^{+}$	6.02	Pot.	35	0.1 M $NaNO_3$				[7]
$Co^{2+} + L^{-} \rightleftharpoons CoL^{+}$	10.98	Pot.	20	0.1 M $NaNO_3$	−101.45	−135.18	−61.16	[7]
$Co^{2+} + L^{-} \rightleftharpoons CoL^{+}$	10.75	Pot.	25	0.1 M $NaNO_3$				[7]
$Co^{2+} + L^{-} \rightleftharpoons CoL^{+}$	10.45	Pot.	30	0.1 M $NaNO_3$				[7]
$Co^{2+} + L^{-} \rightleftharpoons CoL^{+}$	10.10	Pot.	35	0.1 M $NaNO_3$				[7]

$Ni^{2+} + L^{-} \rightleftharpoons NiL^{+}$	11.50	Pot.	20	0.1 M $NaNO_3$	−135.76	−242.59	−63.47	[7]
$Ni^{2+} + L^{-} \rightleftharpoons NiL^{+}$	11.08	Pot.	25	0.1 M $NaNO_3$				[7]
$Ni^{2+} + L^{-} \rightleftharpoons NiL^{+}$	10.75	Pot.	30	0.1 M $NaNO_3$				[7]
$Ni^{2+} + L^{-} \rightleftharpoons NiL^{+}$	10.30	Pot.	35	0.1 M $NaNO_3$				[7]
$Cu^{2+} + L^{-} \rightleftharpoons CuL^{+}$	12.45	Pot.	20	0.1 M $NaNO_3$	−186.9	−399.03	−68.01	[7]
$Cu^{2+} + L^{-} \rightleftharpoons CuL^{+}$	11.96	Pot.	25	0.1 M $NaNO_3$				[7]
$Cu^{2+} + L^{-} \rightleftharpoons CuL^{+}$	11.35	Pot.	30	0.1 M $NaNO_3$				[7]
$Cu^{2+} + L^{-} \rightleftharpoons CuL^{+}$	10.85	Pot.	35	0.1 M $NaNO_3$				[7]
$MnL^{+} + L^{-} \rightleftharpoons MnL_2$	6.70	Pot.	20	0.1 M $NaNO_3$	−375.0	−566.18	−34.51	[7]
$MnL^{+} + L^{-} \rightleftharpoons MnL_2$	6.06	Pot.	25	0.1 M $NaNO_3$				[7]
$MnL^{+} + L^{-} \rightleftharpoons MnL_2$	5.29	Pot.	30	0.1 M $NaNO_3$				[7]
$MnL^{+} + L^{-} \rightleftharpoons MnL_2$	5.0	Pot.	35	0.1 M $NaNO_3$				[7]
$CoL^{+} + L^{-} \rightleftharpoons CoL_2$	7.97	Pot.	20	0.1 M $NaNO_3$	−79.11	−122.92	−42.48	[7]
$CoL^{+} + L^{-} \rightleftharpoons CoL_2$	7.46	Pot.	25	0.1 M $NaNO_3$				[7]
$CoL^{+} + L^{-} \rightleftharpoons CoL_2$	7.21	Pot.	30	0.1 M $NaNO_3$				[7]
$CoL^{+} + L^{-} \rightleftharpoons CoL_2$	6.99	Pot.	35	0.1 M $NaNO_3$				[7]
$NiL^{+} + L^{-} \rightleftharpoons NiL_2$	8.68	Pot.	20	0.1 M $NaNO_3$	−69.46	−70.69	−48.41	[7]
$NiL^{+} + L^{-} \rightleftharpoons NiL_2$	8.50	Pot.	25	0.1 M $NaNO_3$				[7]
$NiL^{+} + L^{-} \rightleftharpoons NiL_2$	8.26	Pot.	30	0.1 M $NaNO_3$				[7]
$NiL^{+} + L^{-} \rightleftharpoons NiL_2$	8.09	Pot.	35	0.1 M $NaNO_3$				[7]
$CuL^{+} + L^{-} \rightleftharpoons CuL_2$	10.20	Pot.	20	0.1 M $NaNO_3$	−162.7	−358.03	−55.92	[7]
$CuL^{+} + L^{-} \rightleftharpoons CuL_2$	9.91	Pot.	25	0.1 M $NaNO_3$				[7]
$CuL^{+} + L^{-} \rightleftharpoons CuL_2$	9.36	Pot.	30	0.1 M $NaNO_3$				[7]
$CuL^{+} + L^{-} \rightleftharpoons CuL_2$	8.81	Pot.	35	0.1 M $NaNO_3$				[7]
4-Bis[(2-hydroxybenzaldehyde)propyl]piperazine (BHPP) (C20)								
$L^{2-} + H^{+} \rightleftharpoons HL^{-}$	10.56	Pot.	25	0.1 M $NaNO_3$				[8]
$HL^{-} + H^{+} \rightleftharpoons H_2L$	9.33	Pot.	25	0.1 M $NaNO_3$				[8]
$H_2L + H^{+} \rightleftharpoons H_3L^{+}$	8.49	Pot.	25	0.1 M $NaNO_3$				[8]
$H_3L^{+} + H^{+} \rightleftharpoons H_4L^{2+}$	7.68	Pot.	25	0.1 M $NaNO_3$				[8]
$Cu^{2+} + L^{2-} \rightleftharpoons CuL$	14.09	Pot.	25	0.1 M $NaNO_3$				[8]
$CuL + H^{+} \rightleftharpoons CuHL$	8.59	Pot.	25	0.1 M $NaNO_3$				[8]
$Ni^{2+} + L^{2-} \rightleftharpoons NiL$	6.74	Pot.	25	0.1 M $NaNO_3$				[8]
$Co^{2+} + L^{2-} \rightleftharpoons CoL$	5.86	Pot.	25	0.1 M $NaNO_3$				[8]
3-(2-hydroxy-3-ethoxybenzylideneamino)-5-methyl isoxazole [HEBMI] (C21)								
$L^{-} + H^{+} \rightleftharpoons HL$	8.58	Pot.	30	0.1 M KNO_3				[87]
$Cu^{2+} + L^{-} \rightleftharpoons CuL^{+}$	6.45	Pot.	30	0.1 M KNO_3				[87]
$CuL^{+} + L^{-} \rightleftharpoons CuL_2$	4.78	Pot.	30	0.1 M KNO_3				[87]

(*Continued*)

Table 1. (*Continued*).

Reaction	log *K*	Method[a]	*T* °C	Medium	Δ*H*°	Δ*S*°	Δ*G*° [b]	Refs.
Sal_2trien (C1)								
$Ni^{2+} + L^{-} \rightleftharpoons NiL^{+}$	5.20	Pot.	30	0.1 M KNO_3				[87]
$NiL^{+} + L^{-} \rightleftharpoons NiL_2$	4.50	Pot.	30	0.1 M KNO_3				[87]
$Co^{2+} + L^{-} \rightleftharpoons CoL^{+}$	4.70	Pot.	30	0.1 M KNO_3				[87]
$CoL^{+} + L^{-} \rightleftharpoons CoL_2$	4.23	Pot.	30	0.1 M KNO_3				[87]
3-(2-hydroxy-5-nitrobenzylidene amino)-5-methyl isoxazole [HNBMI] (C22)								
$L^{-} + H^{+} \rightleftharpoons HL$	6.05	Pot.	30	0.1 M KNO_3				[87]
$Cu^{2+} + L^{-} \rightleftharpoons CuL^{+}$	6.31	Pot.	30	0.1 M KNO_3				[87]
$CuL^{+} + L^{-} \rightleftharpoons CuL_2$	4.75	Pot.	30	0.1 M KNO_3				[87]
$Ni^{2+} + L^{-} \rightleftharpoons NiL^{+}$	4.75	Pot.	30	0.1 M KNO_3				[87]
$NiL^{+} + L^{-} \rightleftharpoons NiL_2$	3.48	Pot.	30	0.1 M KNO_3				[87]
$Co^{2+} + L^{-} \rightleftharpoons CoL^{+}$	4.27	Pot.	30	0.1 M KNO_3				[87]
$CoL^{+} + L^{-} \rightleftharpoons CoL_2$	3.09	Pot.	30	0.1 M KNO_3				[87]
4-(3-methoxy-salicylideneamino)-5-hydroxy-6-(2,5-dichlorophenylazo)-2,7-naphthalene disulfonic acid sodium salt schiff-base ligand (C23) (H_2L)								
$L^{4-} + H^{+} \rightleftharpoons LH^{3-}$	8.82	Pot.	25	0.1 M KCl				[89]
$LH^{3-} + H^{+} \rightleftharpoons LH_2{}^{2-}$	7.35	Pot.	25	0.1 M KCl				[89]
$LH_2{}^{2-} + H^{+} \rightleftharpoons LH_3{}^{-}$	3.89	Pot.	25	0.1 M KCl				[89]
$Cu^{2+} + 2L^{4-} \rightleftharpoons CuL_2{}^{6-}$	23.06	Pot.	25	0.1 M KCl				[89]
$Cu^{2+} + 2L^{4-} + H^{+} \rightleftharpoons CuHL_2{}^{5-}$	7.83	Pot.	25	0.1 M KCl				[89]
$Cu^{2+} + 2L^{4-} + 2H^{+} \rightleftharpoons CuH_2L_2{}^{4-}$	7.76	Pot.	25	0.1 M KCl				[89]
$Cu^{2+} + 2L^{4-} + 3H^{+} \rightleftharpoons CuH_3L_2{}^{3-}$	6.37	Pot.	25	0.1 M KCl				[89]
$Cu^{2+} + 2L^{4-} + 4H^{+} \rightleftharpoons CuH_4L_2{}^{2-}$	3.65	Pot.	25	0.1 M KCl				[89]
$Ni^{2+} + 2L^{4-} \rightleftharpoons NiL_2{}^{6-}$	20.88	Pot.	25	0.1 M KCl				[89]
$Ni^{2+} + 2L^{4-} + H^{+} \rightleftharpoons NiHL_2{}^{5-}$	7.77	Pot.	25	0.1 M KCl				[89]
$Ni^{2+} + 2L^{4-} + 2H^{+} \rightleftharpoons NiH_2L_2{}^{4-}$	6.18	Pot.	25	0.1 M KCl				[89]
$Ni^{2+} + 2L^{4-} + 3H^{+} \rightleftharpoons NiH_3L_2{}^{3-}$	3.47	Pot.	25	0.1 M KCl				[89]
N,N′-bis{2-[(2-hydroxybenzylidine)amino]ethyl}malonamide (BHAEM) (C24)								
$L^{2-} + H^{+} \rightleftharpoons LH^{-}$	8.2	Pot.	25	0.1 M KCl				[90]
$L^{2-} + H^{+} \rightleftharpoons LH^{-}$	8.12	Sp.						[90]
$LH^{-} + H^{+} \rightleftharpoons LH_2$	7.45	Pot.	25	0.1 M KCl				[90]
$LH^{-} + H^{+} \rightleftharpoons LH_2$	7.20	Sp.						[90]
$L\ LH_{1-} + \rightleftharpoons H$	−8.63	Pot.	25	0.1 M KCl				[90]
$L\ LH_{2-} + \rightleftharpoons H$	−17.59	Pot.	25	0.1 M KCl				[90]
$L\ LH_{3-} + \rightleftharpoons H$	−27.90	Pot.	25	0.1 M KCl				[90]
$L\ LH_{4-} + \rightleftharpoons H$	−36.85	Pot.	25	0.1 M KCl				[90]

$Co^{2+} + L^{2-} \rightleftharpoons CoL$	4.67	Pot.	25	0.1 M KCl	[90]
$Co^{2+} + L^{2-} \rightleftharpoons CoL$	3.83	Sp.	25		[90]
$Ni^{i2+} + L^{2-} \rightleftharpoons NiL$	5.04	Pot.	25	0.1 M KCl	[90]
$Ni^{2+} + L^{2-} \rightleftharpoons NiL$	4.95	Sp.	25		[90]
$NiL \rightleftharpoons NiLH_{1-} + H$	−3.06	Pot.	25	0.1 M KCl	[90]
$Cu^{2+} + L^{2-} \rightleftharpoons CuL$	6.86	Pot.	25	0.1 M KCl	[90]
$Cu^{2+} + L^{2-} \rightleftharpoons CuL$	6.18	Sp.	25		[90]
$CuL \rightleftharpoons CuLH_{2-} + 2H$	−6.96	Pot.	25	0.1 M KCl	[90]
$Zn^{2+} + L^{2-} \rightleftharpoons ZnL$	4.80	Pot.	25	0.1 M KCl	[90]
$Zn^{2+} + L^{2-} \rightleftharpoons ZnL$	3.90	Sp.	25		[90]

[a]Method abbreviations are Pot. (potentiometric), Sp. (spectrophotometric), and pH (pH-metrically).
[b]$\Delta H°$ (kJ M^{-1}), $\Delta G°$ (kJ M^{-1}), and $\Delta S°$ (JK^{-1} M^{-1}).

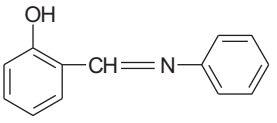

Scheme 5. Structural formula of 2-((phenylimino)methyl)phenol (C2).

2.9.2. SBs derived from salicylaldehyde and aniline. 2-((Phenylimino)methyl)-phenol (C2) (scheme 5) was obtained by mixing equimolar amounts of salicylaldehyde and aniline under reflux conditions for 4 h [56]. The titration curves show that there is one sharp jump indicative of one neutralization equilibrium corresponding to the liberated proton of OH of the aldehydic. The stability constants of divalent Mn, Ni, Cu, and trivalent Cr and Fe with C2 have been determined at 25 °C. An examination of the titration curves indicated that the metal titration curve is lower than the ligand titration curve, indicative of the formation of the complexes. The larger the negative value of $\Delta G°$, the more stable is the complex formed. From table 1, it was observed that complex formation obeyed the order: Cu(II) > Ni(II) > Fe(III) > Cr(III) > Mn(II).

2.9.3. Protonation constants and complex-formation equilibria of SBs derived from salicylaldehyde and p-phenylenediamines. Protonation and complex-formation equilibria of SBs derived from aromatic diamines have received much less attention and thermodynamic data for SB complexes derived from phenylenediamines are limited [43–46, 49]. This can be attributed mainly to insolubility of such compounds in water, which is the most common solvent for potentiometric determination of stability constants, and also to the possible hydrolysis of some compounds to give the starting organic fragments. Thus, the study of these SBs requires the use of an organic or aqueous-organic solvent which can dissolve these compounds.

The protonation constants for SBs derived from o-phenylenediamines H_2sal-o-phen (C3) [44] and H_2sal-4-Cl-o-phen (C4) [57] (scheme 6) have been determined in DMSO–water 80 : 20 (wt/wt) (25 °C; I = 0.5 M $NaClO_4$). Protonation constants have also been reported by Martell *et al.* for 3-F-H_2sal-o-phen (C5) [49] (scheme 6) in dioxane–water 70 : 30 (v/v) (25 °C; I = 0.1 M KCl). The protonation constants of H_2sal-m-phen (C6) [46] have been determined in DMSO–water 80 : 20 (wt/wt) (25 °C; I = 0.1 M $NaClO_4$).

pK_i values for these ligands are listed in table 1. These SBs contain two adjacent weak imine donors and two strongly basic phenolates. Thus, they behave like weak diprotic acids. Only one protonation constant was reported above pH 2.5, indicating the low basicity of the imine nitrogen. The basicity sequence found was: H_2sal-o-phen > H_2sal-4-Cl-o-phen. The lower values of pK_i for H_2sal-4-Cl-o-phen were attributable to electron-withdrawing effect of chloride on the diamine. The pK_i values for 3-F-H_2sal-o-phen [49] are similar to those described above, despite the differences in the solvent, ionic strength, and structural features of the ligands.

The species distribution diagrams as a function of pH for H_2sal-o-phen (figure 1) indicate that from pH 5 to 8, the only existing species is H_2L, whereas in the pH range 9–11 H_2L, HL^- and L^{2-} coexist. The deprotonation is complete at pH > 12 and the only existing species is L^{2-}.

SBs derived from ethylenediamine (H_2salen) and its complexes [47, 48] undergo hydrolytic decomposition in strongly acidic DMSO–water 80 : 20 (wt/wt) solution induced by the

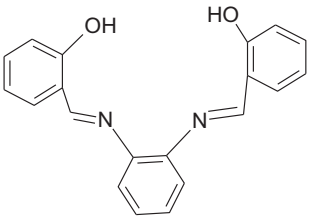

H_2sal-o-phen (C3)

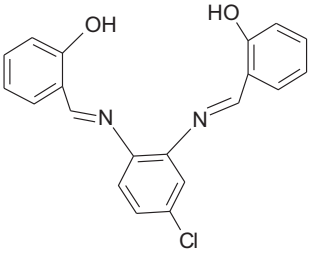

H_2sal-4-Cl-o-phen (C4)

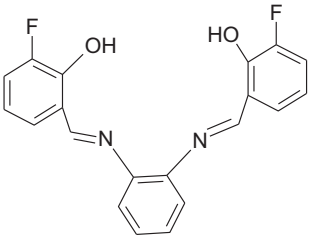

3-F-H_2sal-o-phen (C5)

Scheme 6. Structural formulas of H_2sal-o-phen (C3), H_2sal-4-Cl-o-phen (C4), and 3-F-H_2sal-o-phen (C5).

highly basic character of the nitrogens of the aliphatic diamine; no hydrolysis was observed for SBs derived from ortho- or meta-phenylenediamines in DMSO–water 80 : 20 (wt/wt) above pH 2.5 [44–46]. The low basicity of the nitrogens on the aromatic diamine which remain unprotonated in media where the ethylenediamine is fully protonated is believed to

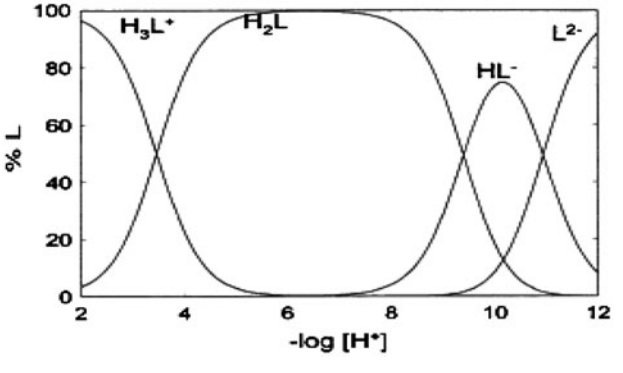

Figure 1. Species distribution diagram for H_2sal-o-phen system.

be responsible for the stability of the SBs and their complexes in acidic DMSO–water solution.

Stability constants have been reported for M-H_2sal-o-phen (M = Ca(II), Mg(II), Fe(III), Ni(II), Co(II), and Zn(II)) [44] and M-H_2sal-4-Cl-o-phen (M = Ca(II), Mg(II), Co(II), and Zn(II)) [57] in DMSO–water 80 : 20 wt : wt (25 °C; I = 0.5 M $NaClO_4$) (table 1). Only $[MHL]^+$ and [ML] were formed (the hydroxo complex [FeOHL] was also observed for the system sal-o-phen-Fe(III)). ML results from coordination of the metal with the fully deprotonated ligand. The monoprotonated complex $[MHL]^+$ may be assumed to be protonated at the phenol oxygen on one salicylaldehyde. The stability of its M(II) complexes for H_2sal-4-Cl-ophen is less than that for H_2sal-o-phen as a consequence of the electron-withdrawing effect of the chloride. Thus, for any metal, the sequence of stability obeys the order H_2sal-o-phen > H_2sal-4-Cl-o-phen, in accord with the basicity order of the SB ligands. ML (M = Fe(III), Ni(II), Co(II), and Zn(II)) is very stable, indicating coordination of both imino groups and the phenolate oxygens. The stability constants for the Ni(II) and Co(II) complexes are similar and slightly higher than those for Zn(II), in agreement with structural data indicating that M–O and M–N bond distances in the solid Ni(II) and Co(II) complexes (average 1.84 and 1.87 Å, respectively) [58] are almost the same. Solutions of Fe(sal-o-phen)Cl in DMSO–water 80 : 20 (wt/wt) are stable and do not undergo any decomposition by addition of strong acids [43]. However, $Fe(salen)^+$ hydrolyses in acidic solutions give salicylaldehyde and ethylenediammonium [59]. The stability of $Fe(sal\text{-}o\text{-}phen)^+$ in acidic media is attributed to the only slightly basic character of o-phenylenediamine.

The stability constants (table 1) for the Ca(II) and Mg(II) with H_2sal-o-phen [44] are considerably smaller than those for the transition metal cations, the Mg(II) species being more stable than the Ca(II). The Mg(II) (smaller in size than Ca(II)) can be better accommodated by the N_2O_2 compartment of the ligand than Ca(II), thus giving more stable species. The stability sequence (table 1) observed for the species ML (H_2L = H_2sal-o-phen) [44, 45] is: Fe(III) > Ni(II) > Co(II) > Zn(II) > Mg(II) > Ca(II). Thus, the Irving–Williams order of complexation which is related to the ligand-field stabilization energy is fulfilled [60].

For M-Sal-o-phen (M = Ni(II), Co(II), and Zn(II)), the species distribution diagram of Ni(II)-salen-o-phen complex as a representative example of M(II)–SB complexes (figure 2) indicates that the neutral ML is the only existing species at pH > 7, so a concentrated solution of ligand : metal ratio 1 : 1 at pH > 7 is the most suitable for the preparation of ML complexes in the solid state. Thus, these complexes are normally prepared in the solid state from the corresponding metal acetate which provides the necessary basic medium.

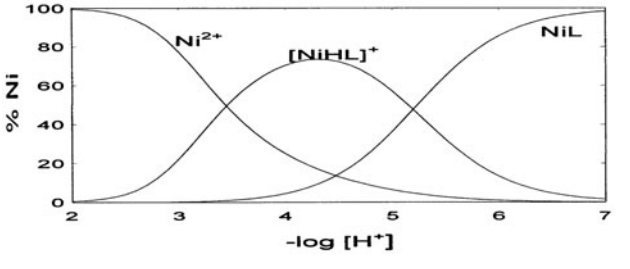

Figure 2. Species distribution diagram as a function of pH for Ni(II)-H_2sal-o-phen at ligand : metal ratio 1 : 1.

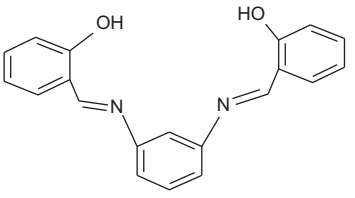

Scheme 7. Structural formula of H_2sal-m-phen (**C6**).

The SB (H_2L) derived from m-phenylenediamines (C6) (scheme 7) formed both monomeric and dimeric species. In the monomeric species $[MHL]^+$ and ML, the metal is coordinated to only one NO of the ligand. For the dimers M_2L_2, both metals are coordinated to a N_2O_2 donor set, in which each NO corresponds to different ligands. The positive values obtained for the dimerization equilibrium $2ML \Leftrightarrow M_2L_2$, indicate a thermodynamically favorable process. The stability sequence found for most species was Cu(II) >> Ni(II) ~ Co(II) > Zn(II). The Irving–Williams order of complexation is thus fulfilled.

By comparing the log K for ML species for H_2sal-m-phen [46] with those corresponding to ML species for H_2sal-o-phen [44], the log K_{ML} for the *meta* SBs are practically half those corresponding to ortho SBs, thus indicating a donor set NO for the former, as expected, due to the conformation of the ligand.

The H_2sal-p-phen SB was first prepared by Pfeiffer and Pfitzner [61] in 1936 by reaction of salicylaldehyde with p-phenylenediamine. No stability constants have been reported to date for SB complexes derived from *p*-phenylenediamines, which is attributed to the insolubility of such compounds in the most common solvents, making formation equilibria very difficult.

2.9.4. Protonation constants and complex-formation equilibria of SBs derived from salicylaldehyde and diaminotoluene. The protonation constants for SBs (H_2L) derived from diaminotoluene have been determined in DMSO–water 80 : 20 (wt/wt) (25°C; I = 0.5 M $NaClO_4$) [46]. The pK_i values for these ligands are listed in table 1. The stability sequence observed for ML (H_2L: H_2sal-2,4-toluene (C7), H_2sal-2,6-toluene (C8)) [46] (scheme 8) is: Cu(II) >> Ni(II) ~ Co(II) > Zn(II) (table 1). Thus, the Irving–Williams order of complexation is fulfilled. The log K order was: H_2sal-2,4-toluene > H_2sal-2,6-toluene.

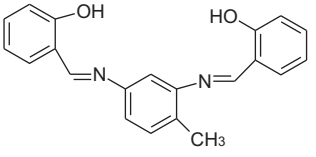

H_2sal-2,4-toluene(C7)

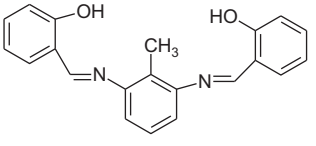

H_2sal-2,6-toluene(C8)

Scheme 8. Structural formula of H_2sal-2,4-toluene (C7) and H_2sal-2,6-toluene (C8).

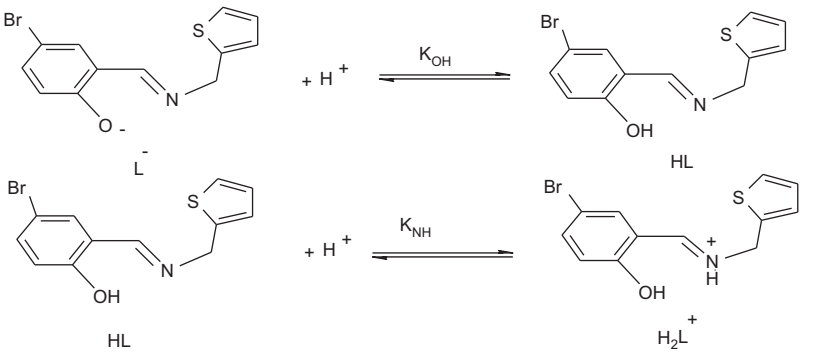

Scheme 9. Protonations of ATS Schiff base (C9).

For complexes derived from H_2sal-2,4-toluene, the inductive electron-donor effect of the methyl group predominates over the repulsive steric effect, in contrast to H_2sal-2,6-toluene.

2.9.5. SBs derived from salicylaldehyde and heteroaromatic amines.

2.9.5.1. Protonation constants and complex-formation equilibria of SB derived from salicylaladehyde and 2-aminomethylthiophene (ATS). Equilibrium studies of 2-aminomethylthiophene and 4-bromosalicylaldehyde Schiff base (ATS) (C9) derived from 2-aminomethylthiophene and 4-bromosalicylaldehyde and their complex formation were determined by potentiometric titration in 50% (v/v) DMSO–water solution at ionic strength of 0.1 M $NaNO_3$ [10]. The stoichiometric protonation constants of ATS in 50% DMSO–water mixture are given in table 1. The two calculated protonation constants are related to protonation of phenolate (log K = 9.96 at 25 °C and I = 0.1 M $NaNO_3$) and imine nitrogen (log K = 5.47 at 25 °C and I = 0.1 M $NaNO_3$), respectively, as shown in scheme 9.

According to the stability constant values given in table 1 [10], the stability order of M(II)–ATS complexes is Zn(II) < Cu(II) > Ni(II) > Co(II) > Mn(II), which is in accord with Irving–Williams order for divalent metals of the 3d series [60, 62].

This is also illustrated in the species distribution of ATS as a function of pH (figure 3), which indicates that in acidic solution ATS initially exists 100% in the fully protonated form as H_2L below pH < 5.5. By increasing the pH, H_2L loses the first proton-forming HL, which is the predominant species from 8.5 to 8.9 with maximum concentration of 90%. As the pH increases further, the second proton begins to deprotonate to L^{2-} reaching a maximum percent of 95% at pH ~ 11.

2.9.5.1.1. Thermodynamics of M(II)–ATS Schiff base. Protonation reaction of the N-site of ATS [10] is exothermic and of comparable $\Delta H°$ and $\Delta S°$ with a net negative $\Delta G°$. The negative $\Delta S°$ indicates that the total number of solvent molecules bound to the dissociated ligand is greater than that originally accompanying the undissociated form. The stability constants of the complexes formed were measured at different temperatures. These values decrease with increasing temperature, confirming that complexation is more favorable at lower temperatures. For ATS at constant temperature, the stability of the chelates is Zn(II) < Cu(II) > Ni(II) > Co(II) > Mn(II) [60, 62]. This order reflects the changes in the

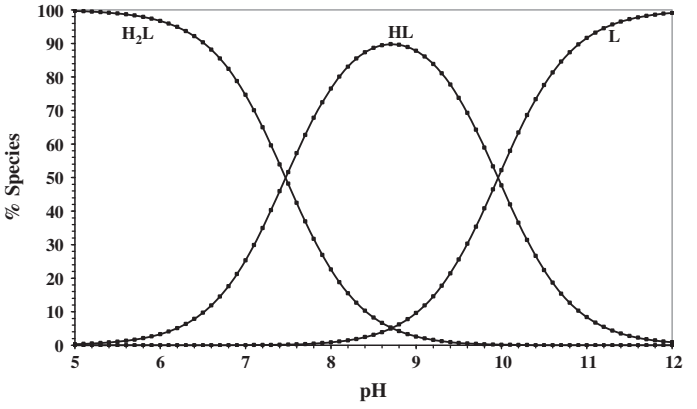

Figure 3. Concentration distribution of various species as a function of pH in the ATS Schiff-base system.

heat of complex formation across the series from a combination of the influence of both the polarizing ability of the metal ion [63] and the crystal field stabilization energies [64]. Stability of the Cu^{2+} complex is higher than those of other metal ions, due to extra stabilization exerted by its d^9 electronic configuration, which is subject to the Jahn–Teller effect. All values of $\Delta G°$ for complexation are negative (table 1), indicating that chelation proceeds spontaneously. Negative values of $\Delta H°$ show that the chelation is exothermic, indicating that complexation reactions are favored at low temperatures. When a coordinate bond between the ligand and the metal ion is formed, the electron density on the metal ion generally increases. Consequently, its affinity for a subsequent molecule ligand decreases, leading to an increase in $\Delta G°$ and $\Delta H°$ of complexation. The entropy term ($\Delta S°$) for complexation is negative, consistent with the protonation reaction of the ligand. The negative entropy changes, together with the high negative enthalpy change, contribute to the favorable free energy change of complex-formation reactions [65].

2.9.5.2. SBs derived from salicylaldehyde and pyridine or its derivatives. For SBs derived from salicylaldehyde and pyridine (salicylidenpyridine-ligands), two protonation constants are calculated. The first refers to protonation of phenolate ion and the second refers to protonation of pyridine. For SAPy (C10), SAPyMe (C11), and SAPyCl (C12) ligands (scheme 10), both protonation constants follow the order SAPyCl < SAPy < SAPyMe. Because of the inductive electron-withdrawing effect of chlorine, the basicity of the pyridine nitrogen in SAPyCl is lower than that of SAPy. On the other hand, the inductive electron-donating effect of the methyl group increases the basicity of the pyridine nitrogen in SAPyMe. The more basic the pyridine nitrogen, the more stable are its proton–ligand complexes.

The complex-formation equilibria can be given as:

$$Ln^{3+} + H_2L^{+} \rightleftharpoons LnL^{2+} + 2\ H^{+}$$

$$LnL^{2+} + H_2L^{+} \rightleftharpoons LnL_2^{+} + 2\ H^{+}$$

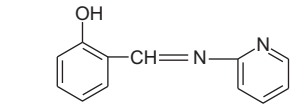

2-((pyridyl-2-imino)methyl)phenol (SAPy)(C10)

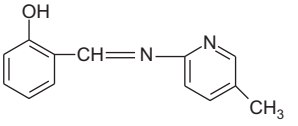

SAPyMe (C11)

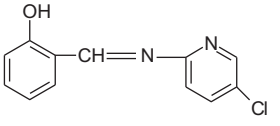

SAPyCl (C12)

Scheme 10. Structural formulas of 2-((pyridyl-2-imino)methyl)phenol (SAPy) (C10), SAPyMe (C11), and SAPyCl (C12).

The stability constants of the lanthanide(III) chelates of all salicylidenpyridine ligands are given in table 1 [66]. The log K_1 values increase in the order La(III) < Pr(III) < Nd(III) < Eu(III) < Ho(III) < Yb(III), which is the order of increasing acidity of the metal ions. The stability constants of the complexes of three salicylidenpyridine ligands with the same metal ion also followed the same order as the proton ligand stability constants of the ligands, i.e. SAPyCl < SAPy < SAPyMe, attributed to the different basicities of the donors of the ligands caused by substituent inductive effects.

The thermodynamic parameters for complexation of the three salicylidenepyridines with metal ions were calculated. The proton–ligand and metal–ligand stability constants decrease with increasing temperature. The negative free energy and enthalpy changes of all the complexes indicated spontaneous and exothermic complexation.

2.9.5.3. SBs derived from salicylaldehyde and 2,3-diaminopyridine. Three protonation constants for SBs C13–C16 (scheme 11) were calculated at 25 °C [67]. K_1 of C13–C16 may be associated with protonation of phenolate, K_2 with protonation of the pyridine and K_3 with protonation of the imino group. The third protonation constant, K_3, determined only for C14 and C15 is related to the imino group at position 3 of the pyridine ring. The imino and amino groups at position 2 of pyridine have too low basicity to allow determination of the corresponding protonation constants. This can be attributed to the fact that protonation constants of the amino group of aminopyridines depend on their substitution site on the pyridine ring [67].

The extremely low basicity of the amino group of 2-aminopyridines is a consequence of the stabilization of the monocation by the resonance equilibrium (scheme 12).

Protonation constants of OH in C13 and C16, having planar structures [68], are $\log K_1$(C13) = 8.82 and log K_1(C16) = 8.75, corresponding to that of salicylaldehyde ($\log K$ = 8.59). The values of the protonation constants of the pyridine nitrogen are $\log K$ = 7.09, showing a significant increase in basicity with respect to unsubstituted pyridine ($\log K$ = 5.34). There is less possibility of delocalization of the negative

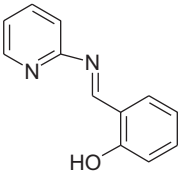

2-(2-pyridyliminomethyl)phenol (C13)

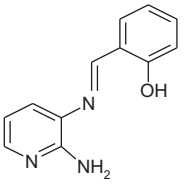

2-(2-amino-3-pyridyliminomethyl)phenol (C14)

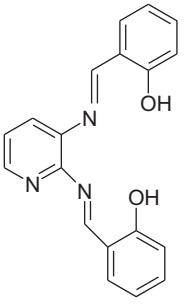

N,N'-bis(salicylidene)-2,3-pyridinediamine (C15)

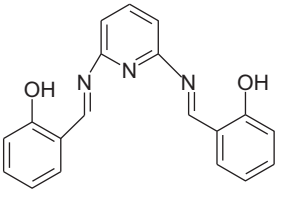

N,N'-bis(sakylidene)-2,6-pyridinediamine (C16)

Scheme 11. Structural formulas of 2-(2-pyridyliminomethyl)phenol (C13), 2-(2-amino-3-pyridyliminomethyl)phenol (C14), N,N'-bis(salicylidene)-2,3-pyridinediamine (C15), and N,N'-bis(sakylidene)-2,6-pyridinediamine (C16).

Scheme 12. Resonance equilibrium of monocation pyridine.

charge through the whole system in C14. In the case of this compound, having a meta-substituted salicylimino on pyridine, X-ray analysis proves that the pyridine ring is tilted by 51.5° with respect to the rest of the molecule [69]. As a consequence, delocalization of the free electron pair of either the phenol oxygen or the amino

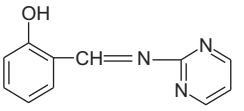

Scheme 13. Structural formula of 2-((pyrimidin-2-ylimino)methyl)phenol (C17).

nitrogen (having a fixed position due to hydrogen bonding of amino protons with the imino nitrogen) is no longer possible. In C15, bearing two salicylimino groups, the first one (2-salicylimino group) has planar orientation to the pyridine ring, whereas the second (3-salicylimino group) is tilted by 51° [69]. Delocalization of the free electron pair is preferred for the 2-salicylimino group as shown by the protonation constant of the pyridine nitrogen ($\log K_2$ = 6.90) similar to the $\log K_2$ value of C16. Although the two hydroxyl groups have different basicity, the difference is too small to allow determination of the protonation constant of each group.

Comparison of protonation constants of C13 (table 1) with the corresponding values ($\log K_1$ = 9.77, $\log K_2$ = 6.37) obtained by potentiometric titration in dioxane–water [70], or $\log K_1$ = 9.3, $\log K_2$ = 7.0 obtained spectrophotometrically in dioxane–water [71], shows differences, explainable by distinctions in experimental conditions, particularly by different solvent composition. In addition to structural effects, solvent effects are factors that influence the basicity of compounds. It was shown that increase in the percentage of organic solvent resulted in an increase in $\log K_{OH}$ and a decrease in $\log K_{NH}$. These changes in protonation constants were related to the decrease in the dielectric constant of the medium, causing better solvation of the neutral species HL than of the charged species L^- and H_2L^+ [72].

2.9.5.4. SBs derived from salicylaldehyde and pyrimidine or its derivatives. The dissociation constants of 2-((pyrimidin-2-ylimino)methyl)phenol (C17) (scheme 13) and the stability constants of the metal complexes Cu(II), Ni(II), Fe(III), Cr(III), and Mn(II) with C17 were determined using both potentiometric and spectrophotometric techniques [73]. From the data given in table 1 for C17, only one equilibrium constant was calculated corresponding to the liberated proton of the OH group of the aldehydic moiety; stability of metal chelates obeyed the order Cu(II) > Ni(II) > Fe(III) > Cr(III) > Mn(II).

Dissociation constants of 4-hydroxysalicylidene-2-amino pyrimidine (H_2sap) (C18) (scheme 13) and the stability constants of the metal complexes Co(II), Ni(II), Cu(II),

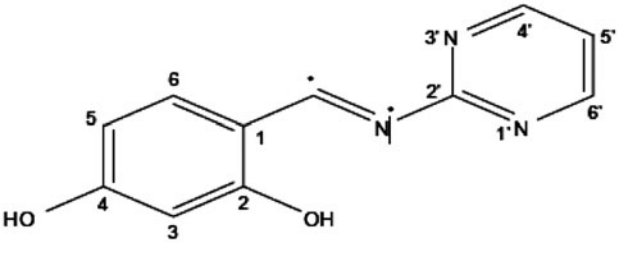

Scheme 14. Structural formula of 4-hydroxysalicylidene-2-amino pyrimidine (H_2sap) (C18).

Pd(II), and Ag(I) with H_2sap were determined pH-metrically at various temperatures at 0.04 mol/L ionic strength of KNO_3, and the thermodynamic reaction parameters ($\Delta S°$, $\Delta G°$, $\Delta H°$) were calculated [74]. The titration curves were below and well separated from that of free H_2sap, confirming complex formation with liberation of protons [75]. From the data given in table 1 [74], log K_1 is higher than log K_2 for the same complex. This can be explained by assuming steric hindrance for the linking of the second species of H_2sap to the central metal ion [76]. The stability constants decreased in the order Cu(II) > Ni(II) > Co(II) for the first-row transition elements in accord with the Irving–Williams order [60, 62].

2.9.5.4.1. Thermodynamics of M(II)–H_2sap (C18) complexes. The thermodynamic parameters of 4-hydroxysalicylidene-2-amino pyrimidine (H_2sap) (C18) are given in table 1. The negative values of $\Delta G°$ indicate spontaneous complex formation [75, 76]. It has been reported that the higher the negative value of $\Delta G°$, the more stable is the complex produced [75–77]. Decrease in stability constants ($\log K_1$ and $\log K_2$) for {Ag(I) and Pd(II)} with increasing temperature suggests that these complex formations are exothermic [75, 78, 79]. For Co(II), Ni(II), and Cu(II), the complex formation is endothermic [79]. The negative values of $\Delta H°$ indicate that the complexation processes are exothermic and favorable at low temperature for both Ag(I) and Pd(II), while the positive values indicate endothermic and favorable at high temperature for Co(II), Ni(II), and Cu(II) complexes. These features support the production of solid Ag(I) and Pd(II) complexes at room temperatures, while those of Co(II), Ni(II), and Cu(II) were isolated after reflux at high temperatures, as reported in the preparation of these complexes [73]. The positive values of $\Delta S°$ indicate that the disorder increased more rapidly than the increase in order taking place in chelation, i.e. the order of arrangement of the solvent around H_2sap and the metal ions are lost upon complexation [79]. In all cases, $\Delta G°$ values are negative, which means that the complexation processes are spontaneous. In comparing $\Delta G°$ values for Co(II), Ni(II), and Cu(II), the value is more negative for Cu(II), suggesting strong interaction between Cu(II) and H_2sap [80].

2.9.5.5. SBs derived from substituted salicylaldehyde and hydralazine. Equilibrium studies of SAH hydrazone (C19) [8] and its complex formation cannot be carried out in aqueous solution because of the nature of the compound involved. Metal complexes as well as SAH hydrazone are insoluble in water, thus DMSO–water mixture was chosen. In such a medium, the hydrazone and its metal complexes are soluble giving stable solutions. The use of this mixed solvent has some advantages over pure DMSO, since pure DMSO is very hygroscopic and controlling its water content is difficult [81], affecting reproducibility of the experiment. However, DMSO–water 70 : 30 has only low hygroscopic character. A further advantage is its compatibility with the standard glass electrode, so that pH measurements may be carried out in a similar way to that employed in purely aqueous solution. In contrast, the use of pure DMSO is not recommended for potentiometry. Another advantage of the DMSO–water mixture is its large acidity range (pK_w = 15.75), which allows the investigation of deprotonation equilibria of weak acids which are difficult to study in water [82, 83]. Stoichiometric protonation constants of the hydrazone were determined in 70% DMSO–water mixture at 25 °C and μ = 0.1 M $NaNO_3$; these constants are given in table 1. Analysis of the potentiometric titration curve of the SAH hydrazone using the Miniquad-75 program gave best fit for two protonation constants as shown in scheme 15. The two protonation constants are related to the protonation of phenolate and phthalazine nitrogen. Titration with a base produces, in a first deprotonation the protonated phthalazine proton

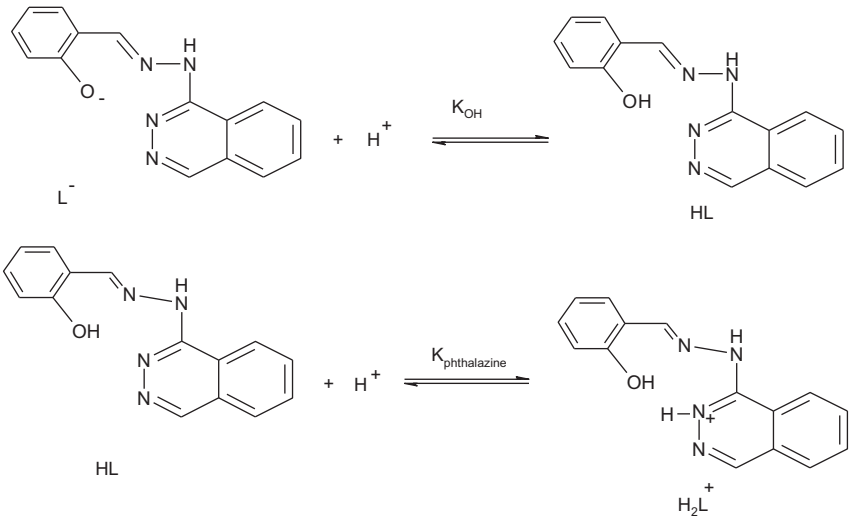

Scheme 15. Protonation of SAH hydrazone (C19).

with a pK_{a1} of 4.35 (pK_{a1} = log β_{012} – log β_{011}). By further increase of pH, the phenolic proton is deprotonated with pK_{a2} of 11.11 (pK_{a2} = log β_{011}) [8].

Potentiometric titrations of SAH with Cu(II), Ni(II), Co(II), and Mn(II) were carried out in 1 : 1 and 1 : 2 metal–ligand molar ratios. Deviation in the metal–ligand titration curves from the ligand titration curve implies formation of metal complexes. The potentiometric titration curve of Ni(II)–SAH as a representative example of metal(II) complexes is given in figure 4.

2.9.5.5.1. Correlation of the properties of metal ions with the formation constants of mixed ligand complexes. To explain why a given ligand prefers binding to one metal rather than another, it is necessary to correlate the stability constants with the characteristic properties of the metal ions, such as ionic radius, ionization energy, electronegativity, and atomic number. Here, we discuss relationships between the properties of metal ions reported in the literature [10, 84] and the stability constants of the complexes. The formation constants of M^{II} complexes of bivalent 3d transition metal ions with SAH as a representative example of SBs are in the order: Cu(II) > Ni(II) > Co(II) > Mn(II), in accord with the Irving–Williams order [8, 60, 62]. Correlation between log K_{ML} and the reciprocal of the ionic radii ($1/r$) of the bivalent transition metal ions was almost linear. Also, a good linear correlation was obtained between log K_{ML} and electronegativities of the metal ions. Increasing electronegativity of the metal ions (Mn(II) (1.55) < Co(II) (1.88) < Ni(II) (1.91) < Cu(II) (2.0)) will decrease the electronegativity difference between the metal and the donor of the ligand. Thus, the metal–ligand bond would have more covalent character, leading to greater stability of the metal chelates. A good linear relationship has been obtained between log K_{ML} and the second ionization potential of the bivalent metal ions. In general, the stability constant of the Cu(II) complex is quite large compared to other metals. The ligand field will give Cu(II) some extra stabilization due to tetragonal distortion of the octahedral symmetry [7, 10, 85, 86]. Thus, log K for the Cu(II) complex deviates significantly when log K values of metal chelates are plotted against properties of the metal ions.

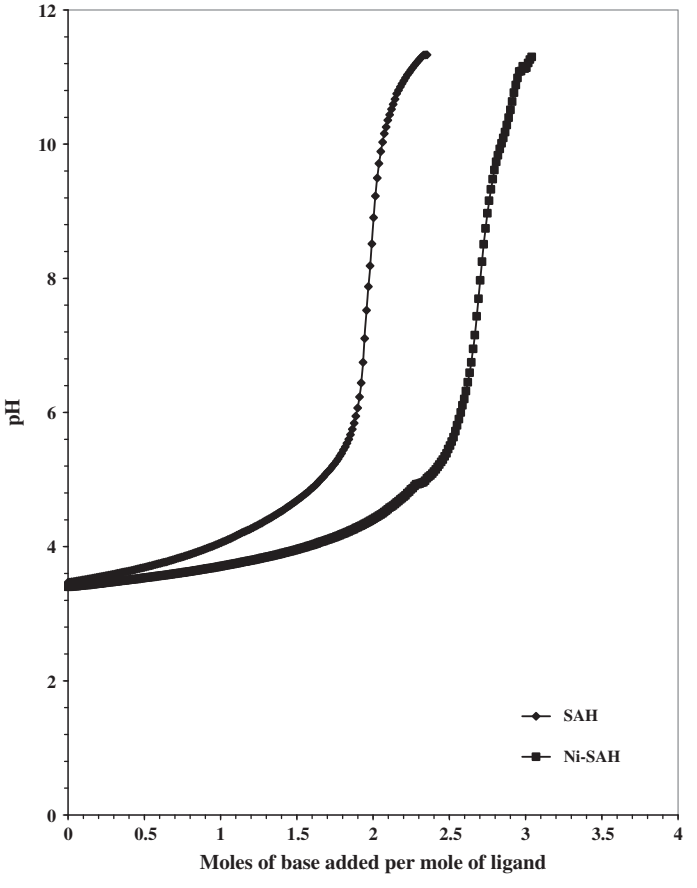

Figure 4. Potentiometric titration curves of Ni-SAH system.

2.9.5.5.2. Thermodynamics of M(II)–SAH complexes. The thermodynamic parameters $\Delta H°$, $\Delta S°$, and $\Delta G°$, associated with protonation of SAH and its complex formation with M (II), were calculated from the temperature dependence of the data in table 1. The protonation reactions of SAH are exothermic with comparable $\Delta H°$ and $\Delta S°$ with a net negative $\Delta G°$. The negative $\Delta S°$ indicates that the total number of solvent molecules bound to the dissociated ligand is greater than that originally accompanying the undissociated form. The stability constants of the complexes were calculated at different temperatures and average values are given in table 1. These values decrease with increasing temperature, confirming that the complexation is more favorable at lower temperatures. The difference between log K_1 and log K_2 is usually positive, since the coordination sites of the metal ions are more available for binding of the first molecule than the second one. The stability of the chelates increases in the order Cu(II) > Ni(II) > Co(II) > Mn(II), reflecting the changes in the heat of complex formation across the series from a combination of the influence of both the crystal field stabilization energies [64] and the polarizing ability of the metal ion [63]. All values of $\Delta G°$ for complexation are negative (table 1), indicating that the chelation proceeds spontaneously. The negative values of $\Delta H°$ show that chelation is exothermic, indicating

that complexation reactions are favored at low temperature. The negative entropy changes, together with the high negative enthalpy change, contribute to favorable free energy change for the complex-formation reactions.

2.9.5.6. SBs derived from salicylaldehyde and 1,4-bis(3-aminopropyl) piperazine (BHPP). The stoichiometric protonation constants of BHPP (C20) (scheme 16) were determined in 50% DMSO–water mixture at 25 °C and these constants are given in table 1 [8]. The BHPP Schiff base has four protonation constants. The species distribution of BHPP is given in figure 5. By increasing the pH, H_4L^{+2} loses a proton-forming H_3L^{+} with the maximum formation degree of 95% at pH 7.9. As pH increases, the second and third protons begin to deprotonate, reaching a maximum percentage of 55% and 67% at pH 8 and 10, respectively. As conditions become more alkaline, the fourth proton begins to deprotonate L^{2-} which is the predominant species at pH > 11. In the potentiometric titration curves of BHPP with metal(II) ions, all metal ions depress the titration curve of the free ligand by release of protons according to the abilities of the metal ions to bind to the Schiff base. To investigate the change in concentration of the metal(II) complexes with pH, the species distribution diagram for Cu-BHPP was examined (figure 6) as a representative example of metal(II) complexes. In the Cu–BHPP distribution diagram, CuHL pre-

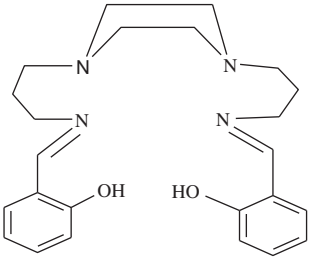

Scheme 16. Structural formula of 4-bis[(2-hydroxybenzaldehyde)propyl]piperazine (BHPP) (C20).

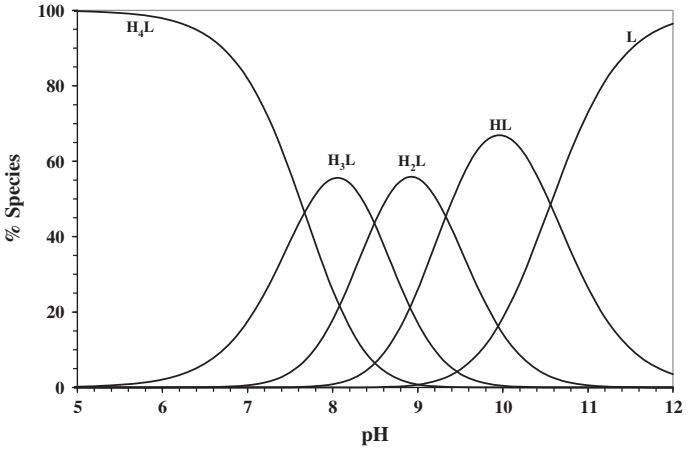

Figure 5. Concentration distribution diagram of BHPP ligand system.

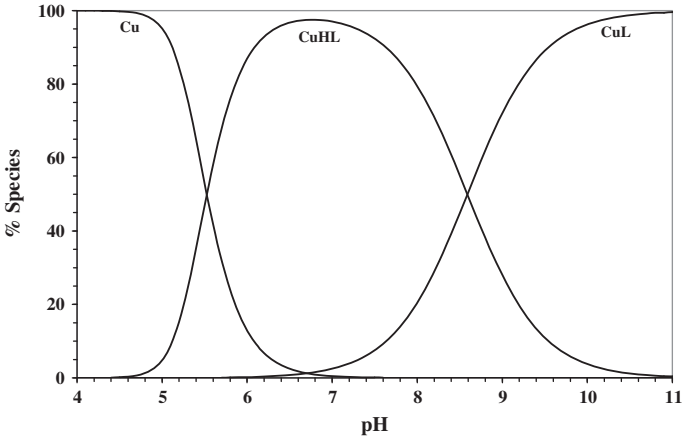

Figure 6. Concentration distribution of various species as a function of pH in the Cu-BHPP system.

dominates in the pH range 6.2–6.8 with a formation percentage of 98%. CuL starts to form at pH 7 and its concentration increases with increasing pH. By examining the values of the stability constants, the magnitude of the stability constant is Cu(II) > Ni(II) > Co(II), in agreement with the Irving–Williams order [60, 62] for divalent metal ions of the 3d series. The stability of the Cu(II) complex is considerably larger than those of other metals of the 3d series. Cu(II) ($3d^9$) receives some extra stabilization due to tetragonal distortion of octahedral symmetry in complexes. The Cu(II) complex will be further stabilized due to the Jahn–Teller effect [62].

2.9.5.7. SBs derived from substituted salicylaldehyde and 3-amino-5-methyl isoxazole. Dissociation constants of SBs, C21 and C22 (scheme 17), and their complex-formation equilibria with some bivalent transition metal ions have been determined potentiometrically in aqueous solution at 30 °C and at 0.1 M KNO_3 ionic strength [87]. The order of stability constants was in accord with the basicity order of the ligands [88]. Stability con-

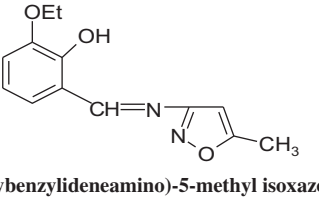

3-(2-hydroxy-3-ethoxybenzylideneamino)-5-methyl isoxazole [HEBMI] (C21)

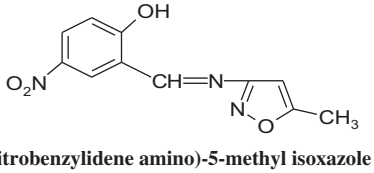

3-(2-hydroxy-5-nitrobenzylidene amino)-5-methyl isoxazole [HNBMI] (C22)

Scheme 17. Structural formulas of 3-(2-hydroxy-3-ethoxybenzylideneamino)-5-methyl isoxazole [HEBMI] (C21) and 3-(2-hydroxy-5-nitrobenzylidene amino)-5-methyl isoxazole [HNBMI] (C22).

stants of C21 are larger than those of C22, attributed to the more basic nature of C21. The stability constants of binary complexes of C21 and C22 with Co(II), Ni(II), and Cu(II) follow the order M(II)–C21 > M(II)–C22. The order of stability with respect to the metal ions is Cu(II) > Ni(II) > Co(II), in accord with the Irving–Williams order.

2.9.6. SBs derived from substituted salicylaldehyde and 4-amino-5-hydroxy-naphthalene-2,7-disulfonic acid. Potentiometric titrations in aqueous solutions were carried out for 4-(3-methoxy-salicylideneamino)-5-hydroxy-6-(2,5-dichlorophenylazo)-2,7-naphthalene disulfonic acid sodium salt (C23) (scheme 18) at 25 °C and 0.1 M KCl. The acidity constants, pK_a (H_2L), for the compounds listed in table 1 differ by at least 4 pK_a units, implying that deprotonation of the second proton is more difficult than releasing the first proton. This difference is caused by formation of an intramolecular hydrogen bond in H_2L. The proton of one of the sulfonic groups is fairly acidic in aqueous media [89] and is deprotonated first. For H_2L, the first constant refers to the deprotonation of the sulfonic group (log K = 3.89) and the second (log K = 7.35) and third (log K = 8.2) constants refer to the deprotonation of the phenolic and naphtholic protons. Species distribution diagrams indicate the best conditions of pH, concentratio,n and ligand : metal ratio for the preparation of the complex in the solid state. From these diagrams, we conclude that a concentrated solution of ligand : metal ratio at various pH is the most suitable for the preparation of ML_2 complex (M = Zn(II), Cu(II), Ni(II), and Co(II)).

2.9.7. SBs derived from salicylaldehyde and N,N′-bis{2-[(2-hydroxybenzylidine)amino] ethyl}malonamide (BHAEM). BHAEM (C24) (scheme 19) was synthesized by condensation of N,N′-bis(2-aminoethyl)malonamide with two equivalents of salicylaldehyde and characterized on the basis of elemental analyses and various spectroscopic measurements (UV–vis, IR, ^{1}H NMR, and ^{13}C NMR) [90]. The protonation constants of diprotic BHAEM (H_2L) were determined by potentiometric and spectrophotometric measurements. Since the ligand was insoluble in water, it was converted into its hydrochloride salt by adding standard 0.1 M HCl to make it water-soluble. For the potentiometric method, the ligand was titrated against standard KOH at an ionic strength of 0.1 M KCl and 25 ± 1 °C in aqueous medium. Six protonation sites (two phenolic groups, two tertiary amines, and two amides) for BHAEM models with LH_n (n = 1−6) were tried for the refinement. However, the best-fit model gave only two protonated species (LH_2 and LH) along with four other species LH_n (n = −1 to −4) in the experimental pH region. The values obtained from the

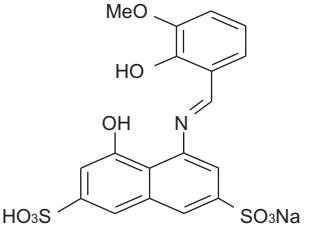

Scheme 18. Structural formula of 4-(3-methoxy-salicylideneamino)-5-hydroxy-6-(2,5-dichlorophenylazo)-2,7-naphthalene disulfonic acid sodium salt schiff-base ligand (C23) (H_2L).

calculation are given in table 1. Previous studies report that the log protonation constants of imine nitrogen of SBs with aromatic diols and triols lie between 1.53 and 2.84 [91] instead of the reported values 3 and 5 [92, 93], which is explained by the fact that substituted phenyls attached to the imine nitrogen inductively reduce the electron density of the imine nitrogen. Accordingly, the protons attached to tertiary amine atoms in BHAEM require very acidic conditions for protonation/deprotonation. Also, the amide nitrogen will require highly basic conditions for deprotonation [94] of the two amide protons. Thus, the two positive protonation constants obtained in the experimental region are assigned to phenolic protons. The values are also in agreement with the protonation constants of other phenols. The simulated titration curve did not fit after $a = 2$ with the experimental curve when only two protonation constants were considered in the model. When four more species, viz. LH_{-1}, LH_{-2}, LH_{-3}, and LH_{-4} were introduced, the simulated curve after $a = 2$ and pH > ~8 matched exactly with the experimental. In the complete mechanism of the hydrolysis of an imine linkage, two moles of H^+ are produced and one mole of BHAEM has two-imine linkages; on hydrolysis, it releases four moles of protons giving species of the type LH_n ($n = -1$ to -4) as observed. The formation of various species is pH-dependent, which is illustrated in the species distribution diagram of BHAEM (figure 7). At pH < 5.0, the ligand exists in the fully protonated form as LH_2. As the pH is increased, the ligand loses two protons from the hydroxyl groups in the aromatic ring to form deprotonated species of the types LH and L, which exist between pH 5.5–9.0 and 7.0–9.5 with maximum concentration of 50 and 40% at pH 7.5 and ~8.4, respectively. Release of protons from the fully deprotonated ligand started after pH 7.5 to give LH_{-1} and, subsequently, in more alkaline medium, gave LH_{-2}, LH_{-3}, and LH_{-4}. LH_{-4} was predominant between pH 9 and 11. This indicates free BHAEM undergoes hydrolysis in alkaline medium. Spectrophotometric titration of BHAEM was also carried out in aqueous solution in acidic and slightly basic media to explain the deprotonation. The spectra were recorded from 210 to 450 nm and between pH 3.94 and 7.98. The equilibrium between the protonated and deprotonated ligand can be examined from the formation of isosbestic points. The spectra passed through five isosbestic points at 220, 243, 265, 289, and 341 nm. Analysis of experimental data by global fitting

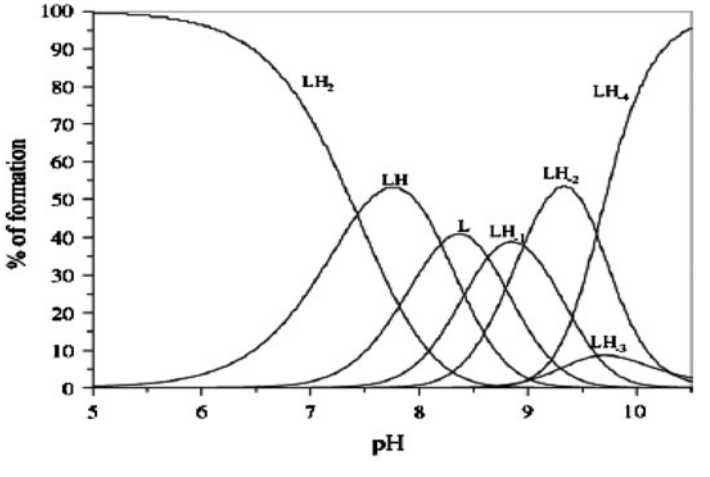

Figure 7. Concentration distribution of various species as a function of pH in the BHAEM system.

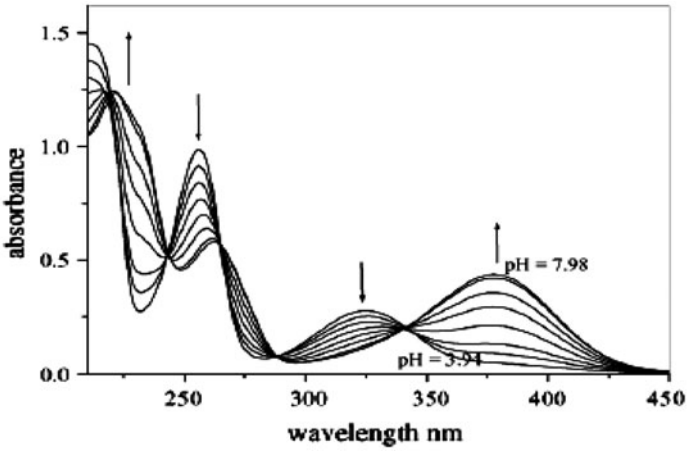

Figure 8. Electronic spectra of BHAEM as a function of pH during a spectrophotometric titration: [BHAEM] = 0.05 mM, [KCl] = 0.1 M, and T = 25 °C.

of the whole spectral data (figure 8) using a non-linear least-square fitting program SPECFIT gave the best fit for the two protonated species. The two protonation constants obtained from the spectrophotometric method (table 1) agree with the result obtained from the

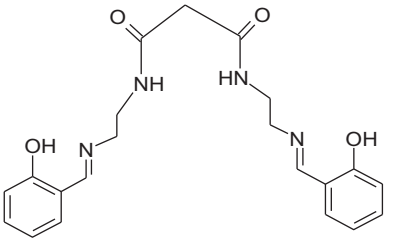

Scheme 19. Structural formula of N,N′-bis{2-[(2-hydroxybenzylidine)amino]ethyl}-malonamide (BHAEM) (C24).

potentiometric method. Inclusion of the hydrolysis model as discussed for the potentiometric method did not give a good fit as there is no hydrolysis in the experimental region of the spectrophotometric study. BHAEM exists predominantly in the enolimine form and is sensitive to hydrolysis in aqueous medium above pH 7.5, before which the phenolic protons dissociate. The protonation constants are ~2.1 log units lower than that of phenol due to intramolecular hydrogen bonding.

2.10. *Amino acid SBs of salicylaldehyde or its derivatives*

Pyridoxal 5′-phosphate (PLP) binds to enzymes to form a Schiff base (imine) by reaction of its aldehyde carbonyl with the terminal ε-amino group of a lysine residue in the polypeptide chain. Metal Schiff-base complexes derived from amino acids (or peptides) play an impor-

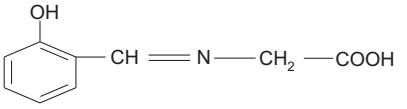

SalGly (C25)

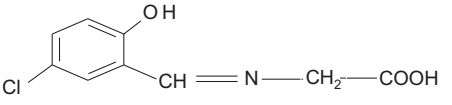

SalCl-Gly (C26)

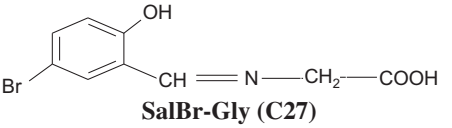

SalBr-Gly (C27)

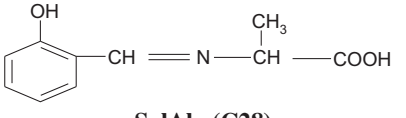

SalAla (C28)

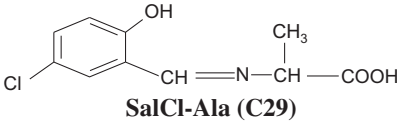

SalCl-Ala (C29)

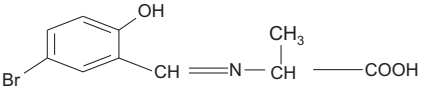

SalBr-Ala (C30)

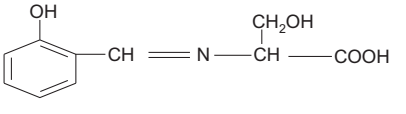

SalSer (C31)

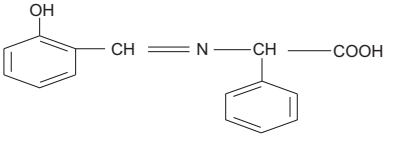

SalPhe (C32)

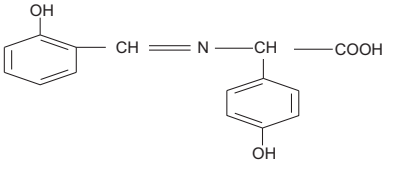

SalTyr (C33)

Scheme 20. Structural formulas of SalGly (C25), SalCl-Gly (C26), SalBr-Gly (C27), SalAla (C28), SalCl-Ala (C29), SalBr-Ala (C30), SalSer (C31), SalPhe (C32), and SalTyr (C33).

Table 2. Equilibrium constants for protonation and complex formation of amino acids and salicylaldehyde or substituted salicylaldehyde amino acid SBs.

Reaction	log K	Method[a]	T°C	Medium	$\Delta H°$	$\Delta S°$	$\Delta G°$[b]	Ref.
SalGly (C25)								
$L^{2-} + H^+ \rightleftharpoons HL^-$	11.68	Pot.	25	0.1 M KCl				[106]
$HL^- + H^+ \rightleftharpoons H_2L$	7.57	Pot.	25	0.1 M KCl				[106]
$H_2L + H^+ \rightleftharpoons H_3L^+$	2.43	Pot.	25	0.1 M KCl				[106]
$Cu^{2+} + L^{2-} \rightleftharpoons CuL$	16.48	Pot.	25	0.1 M KCl				[106]
$Ni^{2+} + L^{2-} \rightleftharpoons NiL$	10.34	Pot.	25	0.1 M KCl				[106]
$NiL + L^{2-} \rightleftharpoons NiL_2^{2-}$	8.36	Pot.	25	0.1 M KCl				[106]
$Zn^{2+} + L^{2-} \rightleftharpoons ZnL$	9.48	Pot.	25	0.1 M KCl				[106]
$ZnL^- + L^{2-} \rightleftharpoons ZnL_2^{2-}$	7.12	Pot.	25	0.1 M KCl				[106]
SalCl-Gly (C26)								
$L^{2-} + H^+ \rightleftharpoons HL^-$	9.60	Pot.	25	0.1 M KCl				[107]
$HL^- + H^+ \rightleftharpoons H_2L$	7.58	Pot.	25	0.1 M KCl				[107]
$H_2L + H^+ \rightleftharpoons H_3L^+$	1.86	Pot.	25	0.1 M KCl				[107]
$Ni^{2+} + L^{2-} \rightleftharpoons NiL$	9.41	Pot.	25	0.1 M KCl				[107]
SalBr-Gly (C27)								
$L^{2-} + H^+ \rightleftharpoons HL^-$	10.74	Pot.	25	0.1 M KCl				[107]
$HL^- + H^+ \rightleftharpoons H_2L$	7.85	Pot.	25	0.1 M KCl				[107]
$H_2L + H^+ \rightleftharpoons H_3L^+$	1.97	Pot.	25	0.1 M KCl				[107]
$Ni^{2+} + L^{2-} \rightleftharpoons NiL$	9.78	Pot.	25	0.1 M KCl				[107]
SalAla (C28)								
$L^{2-} + H^+ \rightleftharpoons HL^-$	11.79	Pot.	25	0.1 M KCl				[106]
$HL^- + H^+ \rightleftharpoons H_2L$	7.42	Pot.	25	0.1 M KCl				[106]
$H_2L + H^+ \rightleftharpoons H_3L^+$	2.40	Pot.	25	0.1 M KCl				[106]
$Cu^{2+} + L^{2-} \rightleftharpoons CuL$	16.98	Pot.	25	0.1 M KCl				[106]
$Ni^{2+} + L^{2-} \rightleftharpoons NiL$	10.10	Pot.	25	0.1 M KCl				[106]
$NiL + L^{2-} \rightleftharpoons NiL_2^{2-}$	8.50	Pot.	25	0.1 M KCl				[106]
$Zn^{2+} + L^{2-} \rightleftharpoons ZnL$	9.05	Pot.	25	0.1 M KCl				[106]
$ZnL + L^{2-} \rightleftharpoons ZnL_2^{2-}$	6.93	Pot.	25	0.1 M KCl				[106]
SalCl-Ala (C29)								
$L^{2-} + H^+ \rightleftharpoons HL^-$	9.69	Pot.	25	0.1 M KCl				[107]
$HL^- + H^+ \rightleftharpoons H_2L$	7.76	Pot.	25	0.1 M KCl				[107]
$H_2L + H^+ \rightleftharpoons H_3L^+$	2.20	Pot.	25	0.1 M KCl				[107]
$Ni^{2+} + L^{2-} \rightleftharpoons NiL$	9.88	Pot.	25	0.1 M KCl				[107]
SalBr-Ala (C30)								
$L^{2-} + H^+ \rightleftharpoons HL^-$	10.25	Pot.	25	0.1 M KCl				[107]
$HL^- + H^+ \rightleftharpoons H_2L$	8.09	Pot.	25	0.1 M KCl				[107]
$H_2L + H^+ \rightleftharpoons H_3L^+$	2.22	Pot.	25	0.1 M KCl				[107]
$Ni^{2+} + L^{2-} \rightleftharpoons NiL$	10.71	Pot.	25	0.1 M KCl				[107]
SalSer (C31)								
$L^{2-} + H^+ \rightleftharpoons HL^-$	11.48	Pot.	25	0.1 M KCl				[106]
$HL^- + H^+ \rightleftharpoons H_2L$	8.0	Pot.	25	0.1 M KCl				[106]
$H_2L + H^+ \rightleftharpoons H_3L^+$	2.15	Pot.	25	0.1 M KCl				[106]
$Cu^{2+} + L^{2-} \rightleftharpoons CuL$	16.72	Pot.	25	0.1 M KCl				[106]
$Ni^{2+} + L^{2-} \rightleftharpoons NiL$	9.99	Pot.	25	0.1 M KCl				[106]
$NiL + L^{2-} \rightleftharpoons NiL_2^{2-}$	8.41	Pot.	25	0.1 M KCl				[106]
$Zn^{2+} + L^{2-} \rightleftharpoons ZnL$	9.85	Pot.	25	0.1 M KCl				[106]
$ZnL + L^{2-} \rightleftharpoons ZnL_2^{2-}$	7.18	Pot.	25	0.1 M KCl				[106]
SalPhe (C32)								
$L^{2-} + H^+ \rightleftharpoons HL^-$	11.93	Pot.	25	0.1 M KCl				[106]
$HL^- + H^+ \rightleftharpoons H_2L$	7.94	Pot.	25	0.1 M KCl				[106]
$H_2L + H^+ \rightleftharpoons H_3L^+$	2.23	Pot.	25	0.1 M KCl				[106]
$Cu^{2+} + L^{2-} \rightleftharpoons CuL$	16.26	Pot.	25	0.1 M KCl				[106]
$Ni^{2+} + L^{2-} \rightleftharpoons NiL$	9.24	Pot.	25	0.1 M KCl				[106]
$NiL + L^{2-} \rightleftharpoons NiL_2^{2-}$	8.06	Pot.	25	0.1 M KCl				[106]
$Zn^{2+} + L^{2-} \rightleftharpoons ZnL$	8.22	Pot.	25	0.1 M KCl				[106]
$ZnL + L^{2-} \rightleftharpoons ZnL_2^{2-}$	6.98	Pot.	25	0.1 M KCl				[106]

(*Continued*)

Table 2. (*Continued*).

Reaction	log *K*	Method[a]	*T*°C	Medium	Δ*H*°	Δ*S*°	Δ*G*°[b]	Ref.
SalTyr (C33)								
$L^{3-} + H^+ \rightleftharpoons HL^{2-}$	12.30	Pot.	25	0.1 M KCl				[106]
$HL^{2-} + H^+ \rightleftharpoons H_2L^-$	9.36	Pot.	25	0.1 M KCl				[106]
$H_2L^- + H^+ \rightleftharpoons H_3L$	7.68	Pot.	25	0.1 M KCl				[106]
$H_3L + H^+ \rightleftharpoons H_4L^+$	2.21	Pot.	25	0.1 M KCl				[106]
$Cu^{2+} + L^{3-} \rightleftharpoons CuL^-$	16.20	Pot.	25	0.1 M KCl				[106]
$Ni^{2+} + L^{3-} \rightleftharpoons NiL^-$	9.26	Pot.	25	0.1 M KCl				[106]
$NiL^- + L^{3-} \rightleftharpoons NiL_2^{4-}$	8.24	Pot.	25	0.1 M KCl				[106]
$Zn^{2+} + L^{3-} \rightleftharpoons ZnL^-$	8.27	Pot.	25	0.1 M KCl				[106]
$ZnL^- + L^{3-} \rightleftharpoons ZnL_2^{4-}$	7.03	Pot.	25	0.1 M KCl				[106]
Glycine (Gly) (C34)								
$L^- + H^+ \rightleftharpoons HL$	9.60	Pot.	25	0.1 M $NaNO_3$				[108]
$HL + H^+ \rightleftharpoons H_2L^+$	11.93	Pot.	25	0.1 M $NaNO_3$				[108]
$Zn^{2+} + L^- \rightleftharpoons ZnL^+$	4.91	Pot.	25	0.1 M $NaNO_3$				[75]
$ZnL^+ + L^- \rightleftharpoons ZnL_2$	9.37	Pot.	25	0.1 M $NaNO_3$				[75]
$Ni^{2+} + L^- \rightleftharpoons NiL^+$	5.78	Pot.	25	0.1 M $NaNO_3$				[109]
$NiL^+ + L^- \rightleftharpoons NiL_2$	10.58	Pot.	25	0.1 M $NaNO_3$				[109]
$Cu^{2+} + L^- \rightleftharpoons CuL^+$	8.19	Pot.	25	0.1 M $NaNO_3$				[110]
$CuL^+ + L^- \rightleftharpoons CuL_2$	14.96	Pot.	25	0.1 M $NaNO_3$				[110]
Alanine (Ala) (C35)								
$L^- + H^+ \rightleftharpoons HL$	9.69	Pot.	25	0.1 M $NaNO_3$				[108]
$HL + H^+ \rightleftharpoons H_2L^+$	11.88	Pot.	25	0.1 M $NaNO_3$				[108]
$Zn^{2+} + L^- \rightleftharpoons ZnL^+$	4.75	Pot.	25	0.1 M $NaNO_3$				[75]
$ZnL^+ + L^- \rightleftharpoons ZnL_2$	8.75	Pot.	25	0.1 M $NaNO_3$				[75]
$Ni^{2+} + L^- \rightleftharpoons NiL^+$	5.41	Pot.	25	0.1 M $NaNO_3$				[109]
$NiL^+ + L^- \rightleftharpoons NiL_2$	9.90	Pot.	25	0.1 M $NaNO_3$				[109]
$Cu^{2+} + L^- \rightleftharpoons CuL^+$	7.99	Pot.	25	0.1 M $NaNO_3$				[110]
$CuL^+ + L^- \rightleftharpoons CuL_2$	14.62	Pot.	25	0.1 M $NaNO_3$				[110]
Phenylalanine (phe) (C36)								
$L^- + H^+ \rightleftharpoons HL$	9.12	Pot.	25	0.1 M $NaNO_3$				[108]
$HL + H^+ \rightleftharpoons H_2L^+$	11.01	Pot.	25	0.1 M $NaNO_3$				[108]
$Zn^{2+} + L^- \rightleftharpoons ZnL^+$	4.30	Pot.	25	0.1 M $NaNO_3$				[75]
$ZnL^+ + L^- \rightleftharpoons ZnL_2$	8.32	Pot.	25	0.1 M $NaNO_3$				[75]
$Ni^{2+} + L^- \rightleftharpoons NiL^+$	5.13	Pot.	25	0.1 M $NaNO_3$				[106]
$NiL^+ + L^- \rightleftharpoons NiL_2$	9.65	Pot.	25	0.1 M $NaNO_3$				[106]
$Cu^{2+} + L^- \rightleftharpoons CuL^+$	7.86	Pot.	25	0.1 M $NaNO_3$				[110]
$CuL^+ + L^- \rightleftharpoons CuL_2$	14.81	Pot.	25	0.1 M $NaNO_3$				[110]
Serine (Ser) (C37)								
$L^- + H^+ \rightleftharpoons HL$	9.14	Pot.	25	0.1 M $NaNO_3$				[111]
$HL + H^+ \rightleftharpoons H_2L^+$	11.40	Pot.	25	0.1 M $NaNO_3$				[111]
$Zn^{2+} + L^- \rightleftharpoons ZnL^+$	4.57	Pot.	25	0.1 M $NaNO_3$				[75]
$ZnL^+ + L^- \rightleftharpoons ZnL_2$	8.49	Pot.	25	0.1 M $NaNO_3$				[75]
$Ni^{2+} + L^- \rightleftharpoons NiL^+$	5.45	Pot.	25	0.1 M $NaNO_3$				[112]
$NiL^+ + L^- \rightleftharpoons NiL_2$	9.69	Pot.	25	0.1 M $NaNO_3$				[112]
$Cu^{2+} + L^- \rightleftharpoons CuL^+$	8.38	Pot.	25	0.1 M $NaNO_3$				[113]
$CuL^+ + L^- \rightleftharpoons CuL_2$	15.45	Pot.	25	0.1 M $NaNO_3$				[113]

[a]Method abbreviations are Pot. (potentiomeric), Sp. (spectrophotometric), and pH (pH-metrically).
[b]Δ*H*° (kJ M^{-1}), Δ*G*° (kJ M^{-1}), and Δ*S*° (JK^{-1} M^{-1}).

tant role for modeling more complicated PLP–amino acid SBs (PLP = pyridoxal-5′-phosphate), as these are key intermediates in a variety of metabolic reactions involving amino acids, such as decarboxylation, transamination, racemization, and C–C bond cleavage, which are catalyzed by enzymes that require PLP as a cofactor [95–97]. Considerable effort has been devoted to the preparation, structural characterization, spectroscopic, and magnetic studies of Schiff-base complexes derived from salicylaldehyde and amino acids [98–103]

and reduced salicylidene amino acid [104, 105], but little attention has been given to the protonation and complex-formation equilibria for these ligands.

2.10.1. Protonation equilibria of amino acid–salicylaldehyde SBs. Protonation and complex-formation equilibria of some SBs (C25–C33) (scheme 20) derived from salicylaldehyde and selected amino acids are given in table 2 [106, 107]. The SBs have three protonation constants as expected. The first refers to protonation of phenolate. The second and third constants correspond to protonation of imine nitrogen and carboxylate, respectively.

The protonation constants of the amino acids [108–114] and the amino acid SBs [106, 107] derived from salicylaldehyde (table 2) indicate that conversion of an amino to an imino group leads to a two-unit decrease in the log K value, as expected, because the sp^2-hybridized N in the –HC = N– would have a less dense negative charge compared to the sp^3-hybridized amine-nitrogen. An equally effective cause for this decrease in basicity could be from the strong intermolecular hydrogen bond between the phenolic OH and the imine nitrogen.

Parallel to this, the base strength of carboxylate sometimes tends to decrease with the transfer of amino acid into a Schiff base. This tendency is attributable to the inductive effect of the more electronegative sp^2 nitrogen. The fact that the change in basicity of the carboxyl site is less by < 0.5 pK units than that observed for the amine–imine change is plausible, since the inductive effects are long-range.

Methyl groups of [SalCl-Ala] and [SalBr-Ala] SBs [107] are capable of releasing electrons, and the electron densities of carboxylate and imine nitrogen increase. Therefore, the second and third protonation constants of these ligands are higher than those for the Gly derivatives. The first protonation constants of the chlorine-substituted SBs are lower than those of the bromine-substituted ones. This can be attributed to the higher inductive electron-withdrawing effect of chlorine.

As the relative pH in most experiments did not extend to pH > 12, the protonation constant for the aliphatic OH in serine could not be measured. However, in its Schiff-base form, this parameter was measurable. That is, the basicity of this group decreases appreciably with formation of the Schiff base. Another qualitative explanation could be based on formation of an intramolecular hydrogen bond as depicted in scheme 21. Assuming that this structure is less favored for the Schiff base due to steric hindrance formed by the aromatic ring, one could argue that the proton on this OH is more difficult to remove in the amino acid form and less difficult in the Schiff base.

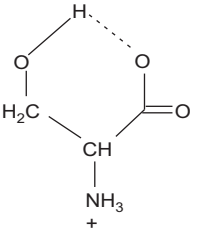

Scheme 21. Intramolecular hydrogen bond in serine amino acid.

2.10.2. Complex-formation equilibria of amino acid SBs. From the data given in table 2, Schiff-base/metal complexes are significantly more stable than the corresponding binary amino acid complexes having the corresponding stoichiometry. The SBs are tridentate ligands, each of which forms five- and six-membered fused two-ring systems. The presence of the bulky group on the α-carbon of the amino acids causes a small, but measurable, decrease in the stability of their Schiff-base complexes. Thus, the order of the stability constants may also be due to steric interactions caused by the bulky group attached to the amino acids.

The stability constants of the complexes with the ligands containing alanine residue are higher than those of the glycine derivatives; the values of the bromine-substituted complexes are higher than the others, as expected, because more stable complexes are formed with stronger bases.

2.11. *Biological aspects of Schiff-base ligands and their metal(II) complexes based on the effect of their stability constants*

In many cases, due to coordination to different transition metal ions in biological systems, it is possible to obtain complexes that are more efficient drugs than the corresponding free ligands [114, 115]. The results of antibacterial and antifungal screening of the SBs and their complexes with bacteria and fungi are given in tables 3–5. Complexes show more activity

Table 3. Antibacterial activity of transition metal complexes.

		Diameter of inhibition zone (in mm)[b]			
Compounds	Parameters	*Pseudomonas aereuginosa*	*Salmonella typhi*	*Bacillus subtillis*	*Staphylococcus aureus*
ATS[a]	$\log K_1^H$ 9.69 $\log K_2^H$ 7.47	12	7	8	8
Ni(II)	$\log K$ 6.65	19	14	14	13
Cu(II)	$\log K$ 9.41	28	16	16	17
Zn(II)	$\log K$ 6.07	23	15	15	15

[a]ATS = 2-Aminomethylthiophenyl-4-bromosalicylaldehyde.
[b]Data taken from Ref. [10].

Table 4. Stability constants and biological activity of ligands and complexes.

Complex	pK_a[b]	$\log K_1$	$\log K_2$	*Escherichia coli*	*Pseudomonas aeurogenosa*	*Rhizopus oryzae*
HEBMI[a]	8.58	–	–	+	+	+
Cu(II)	–	6.45	4.78	+++	+++	++
Ni(II)	–	4.75	3.48	++	++	++
Co(II)	–	4.27	3.09	++	+	++
HNBMI[c]	6.05	–	–	+	+	–
Cu(II)	–	6.31	4.75	+++	++	+++
Ni(II)	–	5.20	4.50	++	++	++
Co(II)	–	4.70	4.23	++	+++	++

[a]3-(2-hydroxy-3-ethoxybenzylideneamino)-5-methyl isoxazole [HEBMI].
[b]Data taken from Ref. [87].
[c]3-(2-hydroxy-5-nitrobenzylidene amino)-5-methyl isoxazole [HNBMI].
Note: Maximum zone of inhibition was represented as +++ (20–35 mm), medium zone of inhibition as ++ (10–20 mm), and minimum zone of inhibition as + (5–10 mm).

Table 5. Protonation constants of amino acid Schiff bases, stability constants of the complexes, and biological activity (zone of inhibition, mm).

Compounds	Parameters[a]		Diameter of inhibition zone (in mm)					
			Bacillus cereus	*Micrococcus luteus*	*Escherichia coli*	*Aeromonas hydrophila*	*Pseudomonas aeroginosa*	*Candida albicans*
SalCl-Gly	$\log K_1^H$	9.60	–	–	–	–	–	–
	$\log K_2^H$	7.58						
	$\log K_3^H$	1.86						
SalCl-Ala	$\log K_1^H$	9.69	–	–	–	–	–	–
	$\log K_2^H$	7.76						
	$\log K_3^H$	2.20						
SalBr-Gly	$\log K_1^H$	10.74	–	–	–	–	–	–
	$\log K_2^H$	7.85						
	$\log K_3^H$	1.97						
SalBr-Ala	$\log K_1^H$	10.25	–	–	–	–	–	–
	$\log K_2^H$	8.09						
	$\log K_3^H$	2.22						
Ni^{II}-SalBr-Ala	$\log K$	10.71	22	6	14	14	14	35
Ni^{II}-SalCl-Ala	$\log K$	9.88	12	6	8	11	8	19
Ni^{II}-SalBr-Gly	$\log K$	9.78	19	8	13	16	14	22
Ni^{II}-SalCl-Ala	$\log K$	9.41	6	4	8	13	12	21

[a]Data taken from Ref. [107].

against different types of bacteria and fungi. Increased activity of the metal chelates can be explained on the basis of chelation theory [116–119]. From data in table 3, for ATS, the antibacterial activity can be ordered as Cu-ATS > Ni-ATS > Co-ATS, suggesting that the lipophilic behavior increases in the same order. This is also in accord with the stability constants order $\log K_{\text{Cu-ATS}} = 9.41 > \log K_{\text{Ni-ATS}} = 6.65 > \log K_{\text{Zn-ATS}} = 6.07$. From data given in table 4, for HEBMI and HNBMI, the Cu(II) complex had a higher biological activity than Co(II) and Ni(II) complexes in accord with the stability order of these complexes. Antifungal and antibacterial screening indicates that Cu^{II} complexes show more activity than other complexes, perhaps from higher stability constant of the Cu^{II} complexes than the other complexes. Activity enhances upon complexation and the order of activity is in accord with the stability order of metal ions [120]. According to the data in table 5, the antibacterial and antifungal activities of the investigated Ni(II) complexes of amino-acid SBs indicated that Ni(II) complexes of higher stability constants are more biologically active than the other Ni(II) complexes.

3. Conclusions

(1) The present review discussed the protonation and complex-formation equilibria of SBs derived from salicylaldehyde or its derivatives. The structure-activity relationships of SBs against bacteria and fungi were discussed based on measured stability constants.

(2) The SBs derived from aliphatic diamines, such as H_2salen, are unstable in acidic aqueous solution because of their hydrolytic decomposition to yield aldehyde and primary amine. However, the Schiff-base H_2sal-o-phen derived from o-phenylenediamine is stable in acidic media and does not undergo decomposition, due to the less basic character of the o-phenylenediamine, which remains unprotonated in the media where the ethylenediamine is completely protonated. This allows thermodynamic studies in the mixed solvent DMSO–water, in which H_2sal-ophen and its complexes are soluble and stable.

(3) Aromatic amines are less basic than aliphatic amines due to the delocalization of the electron pair on the nitrogen towards the orbitals of the aromatic ring, the electron density on nitrogen available for bond formation being lower. Thus, the protonation constants and the stability constants of the ligands derived from aliphatic diamines are larger than those of similar ligands derived from aromatic diamines.

(4) The stability of these complexes, however, is strictly connected with the chelating nature of the ligands, the size of the chelate rings, and the mutual arrangement of all chelate rings in the complexes.

(5) Interesting considerations can be drawn from the contribution of the thermodynamic parameters to complex stability and thus, consideration of the thermodynamic parameters will be important. Negative values of $\Delta H°$ indicate that complexation is exothermic and favorable at low temperature while the positive values indicate endothermic and favorable at high temperature.

(6) The present results may have biological implications. To interpret properly biological processes involving amino acids, it is necessary to have quantitative data on all pertinent equilibrium constants, i.e. the protonation constants of the Schiff base, the stability constants of Schiff-base/metal complexes, and the protonation con-

stants of the amino acids and salicylaldehyde from which the SBs are derived as well as their metal binding constants.

(7) The structure-activity relationship analysis of these SBs based on stability constants suggested that the metal ion plays an important role in the biological activity, *i.e.* metal ions with high stability constants had higher biological activity.

Abbreviations

SBs	generic representation of a Schiff bases
H_2salen	N,N′-ethylenebis(salicylideneimine)
H_2sal-o-phen	N,N′-o-phenylenebis(salicylideneimine)
H_2sal-m-phen	N,N′-m-phenylenebis(salicylideneimine)
H_2sal-p-phen	N,N′-p-phenylenebis(salicylideneimine)
ATS	2-aminomethylthiophenyl-4-bromosalicylaldehyde
o-PDA	o-phenylenediamine
H_2sal-2,4-toluene	N,N′-2,4-toluenebis(salicylideneimine)
H_2sal-2,6-toluene	N,N′-2,6-toluenebis(salicylideneimine)
SAPy	2-((pyridyl-2-imino)methyl)phenol
BHAEM	N,N′-bis{2-[(2-hydroxybenzylidine)amino]ethyl}malonamide
HEBMI	3-(2-hydroxy-3-ethoxybenzylideneamino)-5-methyl isoxazole
HNBMI	3-(2-hydroxy-5-nitrobenzylidene amino)-5-methyl isoxazole
SAH	(2-((2-phthalazin-1-yl)hydrazono)methyl)phenol)
BHPP	1,4-bis[(2-hydroxybenzaldehyde)propyl]piperazine
DMSO	dimethylsulphoxide

References

[1] J. Costamagna, J. Vargas, J. Latorre. *Coord. Chem. Rev.*, **119**, 67 (1992).
[2] A.D. Garnovskii, A.L. Nivorozhkin, V.I. Minkin. *Coord. Chem. Rev.*, **126**, 1 (1993).
[3] A.D. Garnovskii, I.S. Vasil'chenko. *Russ. Chem. Rev.*, **71**, 943 (2002).
[4] R. Eglof, P. Piotr, B. Bogumil, B. Franz. *Curr. Org. Chem.*, **13**, 241 (2009).
[5] G. Ellis, L. Chang, B. Cogionis, D. Daneman. *Clin. Chem.*, **43**, 2437 (1997).
[6] M.K. Khosa, S.A.S. Chatha, M. Nisar, K.M. Zia, K.U. Rehman, M.A. Jamal, M. Yousaf. *J. Chem. Soc. Pak.*, **33**, 421 (2011).
[7] A.A. El-Sherif, M.M. Shoukry, M.M.A. Abd-Elgawad. *J. Spectrochim. Acta (A)*, **98**, 307 (2012).
[8] A.A. El-Sherif, M.R. Shehata, M.M. Shoukry, M.H. Barakat. *J. Spectrochim. Acta (A)*, **96**, 889 (2012).
[9] M.P. Sathisha, U.N. Shetti, V.K. Revankar, K.S.R. Pai. *Eur. J. Med. Chem.*, **43**, 2338 (2008).
[10] A.A. El-Sherif, T.M. Eldebss. *J. Spectrochim. Acta (A)*, **79**, 1803 (2011).
[11] H. Sigel, R.B. Martin. *Chem. Rev.*, **82**, 385 (1982).
[12] J.A. Al-Kandary, F.M.A. Mandani, A.S. Al-Jimaz, A.A. El-Sherif, M.M. Shoukry. *J. Solution Chem.*, **36**, 247 (2007).
[13] B. Jeragh, D. Al-Wahaib, A.A. El-Sherif, A. El-Dissouky. *J. Chem. Eng. Data*, **52**, 1609 (2007).
[14] A.A. El-Sherif. *J. Solution Chem.*, **41**, 392 (2012).
[15] A.A. El-Sherif. *J. Solution Chem.*, **41**, 249 (2012).
[16] A.A. El-Sherif. *J. Coord. Chem.*, **64**, 1240 (2011).
[17] A.A. El-Sherif. *J. Solution Chem.*, **39**, 131 (2010).
[18] A.A. El-Sherif. *Inorg. Chim. Acta*, **362**, 4991 (2009).
[19] F.A. Carey. In *Organic Chemistry*, 5th Edn, p. 724, McGraw-Hill, New York (2003).
[20] G. Wilkinson, R.D. Gillard, J.A. McCleverty (Eds.). *Comprehensive Coordination Chemistry: The Synthesis, Reactions, Properties & Applications of Coordination Compounds*, Pergamon Press, Oxford (1987).
[21] K.N. Campbell, H. Sommers, B.K. Campbell. *J. Am. Chem. Soc.*, **66**, 82 (1944).
[22] J. Hine, C.Y. Yeh. *J. Am. Chem. Soc.*, **89**, 2669 (1976).
[23] H. Tazok, K. Miyano. *J. Chem. Soc.*, 9769 (1959).
[24] C. Munir, S.M. Yousaf, N. Ahmad. *J. Chem. Soc. Pak.*, **7**, 301 (1985).
[25] O. Costisor, W. Linert. *Metal Mediated Template Synthesis of Ligands*, p. 25, World Scientific, Singapore (2004).
[26] L.J. Nunes, G.L. Eichorn. *J. Am. Chem. Soc.*, **84**, 901 (1962).
[27] R.J. Motekaitis, A.E. Martell. *The Determination and Use of Stability Constants*, VCH, New York (1988).

[28] H. Rossotti. *The Study of Ionic Equilibria*, Longman, London (1978).
[29] A.E. Martellm, M. Calvin. *Chemistry of the Metal Chelate Compounds*, Prentice-Hall Inc., New York (1952).
[30] F.C. Rossotti, H. Rossotti. *The Determination of Stability Constants*, McGraw-Hill Inc., New York (1961).
[31] R.G. Bates. *Determination of pH, Theory and Practice*, John Wiley and Sons, New York (1973).
[32] D.J. Legget (Ed.). *Computational Methods for the Determination of Formation Constants*, Plenum Press, New York (1985).
[33] M. Meloum, J. Havel, E. Hgfeldt. *Computation of Solution Equilibria*, Ellis Horwood, Chichester (1994).
[34] R.J. Motekaitis, A.E. Martell. *Can. J. Chem.*, **60**, 3403 (1982).
[35] J. Barbosa, D. Barrn, J. Beltrn, V. SanzNebot. *Anal. Chim. Acta*, **317**, 75 (1995).
[36] A. Sabatini, A. Vacca, P. Gans. *Talanta*, **21**, 53 (1974).
[37] P. Gans, A. Sabatini, A. Vacca. *Inorg. Chim. Acta*, **18**, 239 (1976).
[38] P. Gans, A. Sabatini, A. Vacca. *J. Chem. Soc., Dalton Trans.*, 1195 (1981).
[39] L. Zekany, I. Nagypal. In *Computational Methods for the Determination of Formation Constants*, D.J. Leggett (Ed.), p. 71, Plenum Press, New York (1985).
[40] A. Sabatini, A. Vacca, P. Gans. *Coord. Chem. Rev.*, **120**, 389 (1992).
[41] M. Kılyen, P. Forgo, A. Lakatos, G. Dombi, T. Kiss, N. Kotsakis, A. Salifoglou. *J. Inorg. Biochem.*, **94**, 207 (2003).
[42] M.A. El-Taher, M.T. El-Haty, T.M. Hussien. *Pol. J. Chem.*, **75**, 79 (2001).
[43] F. Lloret, M. Mollar, J. Moratal, J. Faus. *Inorg. Chim. Acta*, **124**, 67 (1986).
[44] R. Hernández-Molina, A. Mederos, P. Gili, S. Domínguez, P. Núñez. *Polyhedron*, **16**, 4191 (1997).
[45] R. Hernández-Molina, A. Mederos, P. Gili, S. Domínguez, P. Núñez, G. Germain, T. Debaerdemaeker. *Inorg. Chim. Acta*, **256**, 319 (1997).
[46] R. Hernández-Molina, A. Mederos, P. Gili, S. Domínguez, F. Lloret, J. Cano, M. Julve, C. Ruiz-Pérez, X. Solans. *J. Chem. Soc., Dalton Trans.*, 4327 (1997).
[47] F. Lloret, J. Moratal, J. Faus. *J. Chem. Soc. Dalton Trans.*, 1743 (1983).
[48] F. Lloret, J. Moratal, J. Faus. *J. Chem. Soc. Dalton Trans.*, 1749 (1983).
[49] R.J. Motekaitis, A.E. Martell. *Inorg. Chem.*, **27**, 2718 (1988).
[50] R.J. Motekaitis, A.E. Martell, D.A. Nelson. *Inorg. Chem.*, **23**, 275 (1984).
[51] M.S. Masoud, F.M. Eizawawy. *Ind. J. Chem.*, **23A**, 149 (1984).
[52] E.S. Jayadevappa, S.C. Galgali. *J. Chem. Soc.*, **LX**, 366 (1987).
[53] G.P. Sengupta, C.R. Bera, N.N. Gosh. *J. Ind. Chem. Soc.*, **LXIV**, 366 (1987).
[54] M. Calligaris, L. Randaccio. In *Comprehensive Coordination Chemistry*, G. Wilkinson (Ed.), Vol. 2, p. 715, Pergamon Press, Oxford (1987).
[55] N. Chantarasiri, V. Ruangpornvisuti, N. Muangsin, H. Detsen, T. Mananunsap, C. Batiya, N. Chaichit. *J. Mol. Struct.*, **701**, 93 (2004).
[56] S.A. Abdel-Latif, H.B. Hassib, Y.M. Issa. *J. Spectrochim. Acta (A)*, **67**, 950 (2007).
[57] A. Mederos, S. Domínguez, R. Hernández-Molina, J. Sanchiz, F. Brito. *Coord. Chem. Rev.*, **193–194**, 857 (1999).
[58] N.B. Pahor, M. Calligaris, P. Delise, G. Dodic, G. Nardin, L. Randaccio. *J. Chem. Soc.*, 2478 (1976).
[59] F. Lloret, M. Mollar, J. Faus, M. Julve, W. Díaz. *Inorg. Chim. Acta*, **189**, 195 (1991).
[60] H. Irving, R.J.P. Williams. *Analyst (London)*, **77**, 813 (1952).
[61] P. Pfeiffer, H. Pfitzner. *J. Prakt. Chem.*, **145**, 243 (1936).
[62] H. Irving, R.J.P. Williams. *J. Chem. Soc.*, 3192, (1953).
[63] F.R. Harlly, R.M. Burgess, R.M. Alcock. *Solution Equilibria*, p. 257, Ellis Harwood, Chichester (1980).
[64] C.S.G. Phillips, R.J.P. Williams. *Inorg. Chem. (Oxford)*, **2**, 268 (1966).
[65] A.A. El-Sherif, M.M. Shoukry, M.A. Abd El-Gawad. *J. Solution Chem.*, **42**, 412 (2013).
[66] P. Gürkan, N. Sari. *Talanta*, **44**, 1935 (1997).
[67] N. Galić, Z. Cimermana, V. Tomišić. *Anal. Chim. Acta*, **343**, 135 (1997).
[68] Z. Cimerman, N. Gale, B. Bosner. *J. Mol. Struct.*, **274**, 131 (1992).
[69] Z. Cimerman, N. Kiralj, N. Galid. *J. Mol. Struct.*, **323**, 7 (1994).
[70] Z. Holzbecher, H. van Trung. *Collect. Czech. Chem. Commun.*, **41**, 1507 (1976).
[71] W.J. Geary, G. Nickless, F.H. Pollard. *Anal. Chim. Acta*, **27**, 71 (1962).
[72] T. Gilndiiz, E. Kilic, E. Cane. *Anal. Chim. Acta*, **282**, 489 (1993).
[73] S.J. Angyal, C.L. Angyal. *J. Chem. Soc.*, 1461 (1952).
[74] A. Ouf, M.S. Ali, E.M. Saad, S.I. Mostafa. *J. Mol. Struct.*, **973**, 69 (2010).
[75] A.A. El-Sherif. *J. Solution Chem.*, **39**, 1562 (2010).
[76] M. Aljahdali, A.A. El-Sherif. *J. Solution Chem.*, **41**, 1759 (2012).
[77] B. Jeragh, D. Al-Wahaib, A.A. El-Sherif, A. El-Dissouky. *J. Chem. Eng. Data*, **52**, 1609 (2007).
[78] S. Saeeduddin, A. Khanzada. *Pak. J. Pharm. Sci.*, **17**, 83 (2004).
[79] A. El-Bindary, I. Shehatta. *Monatsh. Chem.*, **125**, 841 (1994).
[80] I.M.M. Kenawy, M.E.M. Emam, M.A.H. Hafez. *Thermochim. Acta*, **188**, 25 (1991).
[81] H. Koksal, M. Dolaz, M. Tumer, S. Serin. *Synth. React. Inorg. Met.-Org. Chem.*, **31**, 1141 (2001).

[82] D. Martin, H.G. Hauthal. *Dimethyl Sulphoxide*, Van Nostrand Reinhold, Workingham (1975).
[83] R. Hernandez-Molina, A. Mederos, P. Gili, S. Dominguez, P. Nunez, G. Germain, T. Debaerdemaeker. *Inorg. Chim. Acta*, **256**, 319 (1997).
[84] J.E. Huheey. *Inorganic Chemistry*, SI Edn, Harper, New York (1983).
[85] M.T. Beck. *Chemistry of Complex Equilibria*, Akademiai Kiado, Budapest (1970).
[86] F.A. Cotton, G. Wilkinson. *Inorg. Chem.*, Wiley, London (1962).
[87] Y. Prashanthi, K. Kiranmai, N.J.P. Subhashini, Shivaraj. *J. Spectrochim. Acta (A)*, **70**, 30–35 (2008).
[88] A.A. El-Sherif. In *Stoichiometry and Research, "The Importance of Quantity in Biomedicine". "Coordination Chemistry of Palladium(II) Ternary Complexes with Relevant Biomolecules"*, Chap. 4, p. 79, In-Tech Publisher, Rijeka (2012).
[89] M. Tunçel, H. Sari. *Transition Met. Chem.*, **32**, 803 (2007).
[90] S.K. Sahoo, S.E. Muthu, M. Baral, B.K. Kanungo. *J. Spectrochim. Acta (A)*, **63**, 574 (2006).
[91] A. Golcu, M. Tumer, H. Demirelli, R.A. Wheatley. *Inorg. Chim. Acta*, **358**, 1785 (2005).
[92] H. Doine. *Bull. Chem. Soc. Jpn.*, **58**, 1327 (1985).
[93] T. Gunduz, E. Kilic, F. Koseoglu, E. Canel. *Anal. Chim. Acta*, **282**, 489 (1993).
[94] The Predicted Value of pKa was Obtained using the ACD/I-Lab Web Service (ACD/pKa 6.0), Advanced Chemistry Development, Inc.
[95] R.F. Zabinski, M.D. Toney. *J. Am. Chem. Soc.*, **123**, 193 (2001).
[96] S.D. Wetmore, D.M. Smith, L. Radom. *J. Am. Chem. Soc.*, **123**, 8678 (2001).
[97] Y. Bkouche-Waksman, J.M. Barbe, A. Kvick. *Acta Crystallogr. B*, **44**, 595 (1988).
[98] S. Mondal, P. Ghosh, A. Chakravorty. *Inorg. Chem.*, **36**, 59 (1997).
[99] D. Leibler, A. Rabinkov, M. Wilchek. *J. Mol. Recognit.*, **9**, 375 (1996).
[100] R. Karmakar, C.R. Choudhury, S. Mitra, L. Dahlenburg. *Struct. Chem.*, **16**, 611 (2005).
[101] B. Baruah, S. Das, A. Chakravorty. *Inorg. Chem.*, **41**, 4502 (2002).
[102] J. Costa Pessoa, I. Tomaz, T. Kiss, P. Buglyó. *J. Inorg. Biochem.*, **84**, 259 (2001).
[103] A. Garcia-Raso, J.J. Fiol, F. Badenas, E. Lago, E. Molins. *Polyhedron*, **20**, 2877 (2001).
[104] C.T. Yang, B. Moubaraki, K.S. Murray, J.D. Ranford, J.J. Vittal. *Inorg. Chem.*, **40**, 5934 (2001).
[105] R. Ganguly, B. Sreenivasulu, J.J. Vittal. *Coord. Chem. Rev.*, **252**, 1027 (2008).
[106] H. Demirelli, F. Köseoğlu. *J. Solution Chem.*, **34**, 561 (2005).
[107] N. Saria, P. Gürkana, S. Çete, I. Şakiyan. *Russ. J. Coord. Chem.*, **32**, 511 (2006).
[108] A.A. El-Sherif. *J. Solution Chem.*, **35**, 1287 (2006).
[109] G. Gran. *Acta Chem. Scand.*, **4**, 559 (1950).
[110] A.A. El-Sherif, M.M. Shoukry. *J. Coord. Chem.*, **58**, 1401 (2005).
[111] A.A. El-Sherif, M.M. Shoukry. *J. Spectrochim. Acta (A)*, **66**, 691 (2007).
[112] D.D. Perrin, W.L.F. Armarego, *Purification of Laboratory Chemicals*, 3rd Edn, Pergamon, Oxford (1980).
[113] M.M. Shoukry, E.M. Khairy, A.A. El-Sherif. *Transition Met. Chem.*, **27**, 656 (2002).
[114] R.P. John, A. Sreekanth, V. Rajakannan, T.A. Ajith, M.R.P. Kurup. *Polyhedron*, **23**, 2549 (2004).
[115] M. Belicchi-Ferrari, F. Bisceglie, C. Casoli, S. Durot, I. Morgenstern-Badarau, G. Pelosi, E. Pilotti, S. Pinelli, P. Tarasconi. *J. Med. Chem.*, **5**, 1671 (2005).
[116] N. Raman, A. Kulandaisamy, A. Shanmugasundaram, K. Jeyasubramanian. *Transition Met. Chem.*, **26**, 131 (2001).
[117] R.S. Srivastava. *Inorg. Chim. Acta*, **56**, 65 (1981).
[118] N. Gupta, R. Swaroop, R.V. Singh. *Main Group Met. Chem.*, **14**, 387 (1997).
[119] A.C. Ukurovali, I. Yilmaz, H. Özmen, M. Ahmedzade. *Transition Met. Chem.*, **27**, 171 (2002).
[120] M. Robert, R.J. Motekaits, A.E. Martell. *Inorg. Chim. Acta*, **103**, 73 (1985).